University of Naples Federico II

International PhD program on
NOVEL TECHNOLOGIES FOR MATERIALS, SENSORS AND IMAGING
XXVIII cycle

PhD School in Industrial Engineering

PhD Thesis

Fabrication of microdevices for biomedical applications based on lithographic approach

Alessandro Caliò

Supervisor: Dr. Luca De Stefano

Institute for Microelectronics and Microsystems

National Council of Research

A mio nipote Tommaso e alle mie nipoti Alice, Nicole e Rebecca.

Table of contents

1. Introduction

Health care and devices used to delivery and monitor health are unquestionably among the most important and critical elements in our society today, and they will continue to become even more important in the future as the world population grows, and the demand for improved quality and more diverse distribution of health services delivered increases. During the past few decades, significant improvements were done in understanding the origin of various diseases, in development of new and exciting tools to fight and detect diseases, and obviously in cost of delivering health care. Prevention and treatment are equally important as our society moves into the twenty first century, and these show an ever increasing need for better equipment and facilities to assist in delivering the highest quality health care. These equipments need to provide the highest performance at the lowest possible cost. In spite of significant progresses made in both of these areas, today there are serious limitations imposed on our health care delivery due to very high costs involved. Any new technology that can help reduce this cost will undoubtedly find a significant market and will lay the foundation for the development of a new generation of biomedical systems. A possible roadmap leads to the realization of biomedical devices and systems using microfabrication processes, traditionally used for manufacture integrated circuits.

Microfabrication processes have revolutionized pharmaceutical, medical and biological fields since they offer the possibility for highly reproducible mass fabrication of systems with complex geometries and functionalities, including novel drug delivery systems and bionsensors (Betancourt et al., 2006). Microdevices, realized using microfabrication processes, have many advantages over their macroscale counterparts. For instance, miniaturization allows manufacturing of portable, hand-held, implantable or even injectable microdevices. In addition, as a result of their minute size, these microdevices need less sample or reagent for analysis or operation, saving money and time. Moreover, where materials and/or processes are inhibited by lengthy diffusion times, miniaturization provides a mechanism for shortening these ones. A notable example where these microdevices allow for significant advantages over traditional counterparts is in medical care: point of care diagnostic testing, which is testing performed at the patient's bedside, permits physicians to diagnose a patient's conditions more rapidly than conventional lab based testing. By using these microdevices to reduce the time of diagnoses, the physician is able to make better patient management decisions leading to improved patient outcomes and reduce the overall cost of care. The basic microfabrication process is based on deposition, patterning, doping and

etching steps (Sze, 2008). Deposition consists in placing a thin layer (or film), such as an insulating silicon dioxide layer, on a substrate, such as a silicon wafer, using chemical or physical process. A light-sensitive resist, called photoresist, is then deposited on the top of the thin layer and patterned using photolithography (or optical lithography). Finally, the pattern is transferred from the photoresist layer to the thin layer by dry or wet etching process. After removing the remaining photoresist, a next layer can be deposited and structured, and so on. Doping of a semiconductor material, such as silicon, by ion implantation or diffusion process can be done directly after photolithography. Traditionally, silicon, glass and ceramics are used as substrates, dielectric, metal and polycrystalline silicon are used as thin layers and some particular commercial polymers, such as SU-8, are used as photoresists. These materials are commonly called hard materials and show superior mechanical properties which make them suitable for the realization of a large variety of microdevices (microprocessors, accelerometers, and so on). Microfabrication processes, and related materials, were developed for applications in the semiconductor industry and are, consequently, not specific for biological, medical and other applications. In some fields, such as biological and biomedical, the use of the hard materials is not the more suitable choice (Quake et al., 2000). For example, many biomedical applications require delicate surface chemistry that is difficult to achieve with high temperatures required to bond silicon and glass. The so called soft materials, mostly based on polymers, such as hydrogel, polydimethylsiloxane (PDMS), norland optical adhesive (NOA), can be used to overcome many of the limitations of the hard materials. Polymers are inexpensive, biocompatible therefore provide a more suitable interface with biological tissue, reducing irritation and scarring, and can be used in disposable devices. A specific group of fabrication processes, called soft lithography, was developed to realize microdevices using soft materials (Gates et al., 2005; Lipomi et al., 2012). Some of them are microcontact printing, microtransfer molding and replica molding. The combination of hard materials and processes with soft ones allows to benefit from the advantages of both, providing the realization of microdevices with functionalities that are difficult to achieve with only hard materials and processes or only soft ones. Microfabricated devices, like microelectromechanical systems (MEMS), lab-on-a-chip (LoC) and micro-total analysis systems (micro-TAS), have been designed for more than thirty years, but only in the last few years they are gaining great success. High throughput, small sample volumes, high surface-area-to-volume ratio, commercially scale-up and so on demands in several fields, like biology and chemistry, have created a need for these devices. Interest in using MEMS for *in vivo* applications is started in the 1990s in the academic world. Biomedical

microelectromechanical systems (BioMEMS) are now a heavily researched area with a wide variety of important biomedical applications. In general, BioMEMS can be defined as devices or systems, constructed using techniques inspired from micro/nano-scale fabrication, used for processing, delivery, manipulation, analysis, or construction of biological and chemical entities. Most of the activities in the BioMEMS area are moving towards commercialization of these biomedical devices and systems (Ziaie et al., 2004). For example, a MEMS based DNA sequencer developed by the Cepheid is currently being installed in post offices across USA for bioagent detection. BioMEMS drug delivery systems are also actively targeted by many investigators and companies as is evident, for example, from current efforts by MicroCHIPS, to commercialize an electronically activated drug delivery microchip, by ChipRx, to introduce systems that integrate silicon and electroactive polymer technologies for controlled delivery, and by iMEDD, to develop nanoporous membranes and micromachined particles for a variety of drug delivery applications. Large efforts are dedicated to realize others commercial BioMEMS, such as microneedles based devices for transdermal drug delivery and transdermal biosensing, and microfluidic device for microdialysis.

The aim of the scientific research investigated in these three years of PhD course is to define the fabrication procedures, based on lithographic processes on both hard and soft materials, for the realization of innovative microdevices for biomedical applications. In particular, microneedles based devices for drug delivery and biosensing, and device for microfluidic filtration have been explored.

Microneedles are three-dimensional structures and represent the interface between a device and the patient's body for extracting, sampling or releasing physiological fluid. The length of microneedles should be long enough that they can penetrate epidermis and short enough not to reach dermis, in order to avoid any pain. The concept of microneedles was proposed in the 1970s, but it was not realized experimentally until the 1990s when the industry of microelectronics provided the microfabrication tools essential to make such small structures. Microfabrication processes are the most promising to fabricate optimal microneedles for any application. The first microneedle arrays reported in literature were developed by etching the silicon wafer for intracellular delivery (Campbell et al., 1991). These needles were inserted into cells and nematodes to increase molecular uptake and gene transfection. After that, a number of attempts were made by various researchers to develop different designs. Several categories of microneedles were reported in literature for various applications. Microneedles can be categorized on the basis of the shape (cylindrical, conical, pyramidal, etc) (Ashraf et al., 2010) and feature (solid, hollow, dissolving, etc) (Chandrasekaran, 2003; Sachdeva et al.,

2011). Microneedles can also be classified on the basis of materials (Ashraf et al., 2010), depending on application. Most of researchers used silicon for microneedles fabrication (Wilke et al., 2005; Ashraf et al., 2010), since it is inexpensive, of high purity and there are a lot of fabrication procedures, coming from the microelectronics industry, able to manipulate this material. However, silicon is a brittle material and can be harmful to health. Different researchers have understood this critical issue and shifted to soft materials. Fabrication of microneedles were reported using various soft materials such as polyglycolic acid (PGA), poly(methyl methacrylate) (PMMA), PDMS, and so on (Aoyagi et al., 2008; Kochhar et al., 2013). Typical lengths of microneedles are in the range of 100-300 µm for drug delivery (Ashraf et al., 2010; Chen et al., 2010), 1100-1600 µm for blood extraction (Tsuchiya et al., 2005). Various fabrication techniques/processes were developed and used for microneedles fabrication such as hot embossing (Oh et al., 2008), laser micromachining (Bhandari et al., 2008), micromolding (Lee et al., 2008), coherent porous silicon etching (Rajaraman et al., 2005), photolithography (Shibata et al., 2007). Currently, the most important application areas of microneedles can be considered transdermal drug delivery and transdermal biosensing.

Development of functional delivery systems for active pharmaceutical ingredients is a challenging task. Drugs can be administered through most common routes like oral, parenteral and transdermal route, as well as less explored routes such as nasal, pulmonary and buccal (Langer, 2001). Each of these routes has specific pros and cons. Oral drug delivery systems offer advantages such as patient compliance, large surface area with rich blood supply for absorption, low cost, easiness in engineering of drug release in stomach/intestine. However, limitations, such as drug degradation in gastrointestinal tract, first pass metabolism, poor absorption, local irritation and variability in absorption (due to factors like pH, motility, food, mucus layer), are associated with these drug delivery systems. The parenteral route offers advantages like quick onset of action, accurate drug delivery and continuous drug delivery by infusion. Its major limitations include pain associated with the injections, expertise required to drug deliver, risk of infection and difficulty in obtaining sustained drug delivery. Transdermal drug delivery involves the transport of drug across the skin. Optimal physiochemical properties are required in drug candidates for delivery via transdermal patches. Transdermal drug delivery offers advantages like patient compliance, avoidance of first pass metabolism, large surface area of skin over which to deliver the drug, quick termination of dosing. However, only a few products with optimum characteristics were successfully marketed to deliver a drug through the skin. Skin can be divided into three regions: 1) the outer most cellular layer, called epidermis, which contains the stratum corneum; 2) the middle layer,

called dermis; 3) the inner most layer, called hypodermis. Skin varies in thickness, according to anatomic site and age of individual. The epidermis layer, whose thickness varies between 50 and 150 μm, is made up of viable cells without a vascular network. This layer obtains its nutritional needs by passive diffusion through interstitial fluid. The outermost layer of the epidermis, that is the stratum corneum (20-40 μm), consists of dead cells, which act as a hard barrier. The dermis, an integrated fibro-elastic structure that has a thickness of about 500-2000 μm, provides mechanical strength to the skin. This layer contains an extensive nervous and vascular network. The pain associated with parenteral drug delivery is due to possible damage to the nerves endings within the dermis. For drug delivery across the skin, the challenge is to cross the intact stratum corneum layer without causing damage to nerves endings. Only a few potent drug molecules, with high lipophilicity and small molecular weight (< 500 Da), can be administered directly through passive diffusion (Matteucci et al., 2008). Various chemical and physical approaches were employed to improve drug penetration across the skin (Milewski et al., 2010). Chemical approaches include use of penetration enhancers, like surfactants, fatty acids/esters and solvents to dissolve the stratum corneum lipid or to increase the solubility of drugs. Physical approaches, like electroporation, ionphoresis, magnetophoresis and sonophoresis, were found suitable to create pathways for only few drugs across the skin. The aforementioned approaches are associated with certain drawbacks: chemical approaches are often associated with higher skin irritation and are applicable only to small molecules, while physical methods typically require a device with a power supply which adds to the cost and complexity. Searching for inexpensive and reliable way to administer the drug safely to the epidermal layer without damaging the nerve cells of dermis, and minimizing chances of microbial penetration, led to the development of microneedles (Donnelly et al., 2009).

Integration of biorecognition and signal transduction elements is an important area of biosensors research. Analytical devices combining the specificity of biological systems with the advantages of electrochemical transduction have gained an increased popularity in the last two decades. Enzymatic redox reactions are particularly amenable to be interfaced with electrochemical transducers, since electron exchange is a key step in their natural cycle. In general, enzymes can operate in liquid environments or immobilized on various supports. Immobilized means that the enzyme is unable to move, but the enzyme activity still remains in the analytical device, although in a generally minor extension when compared with free enzymes. The main advantages of enzymes immobilized on supports compared to free enzymes systems are reduction of costs of operations, higher enzyme stability, ability to stop

the reaction rapidly by simply removing the enzyme from the reaction solution, the fact that products are not contaminated with the enzyme and the possibility of establishing a model system to study enzyme action with variable applications. Enzyme based electrodes are an important class of biosensors where by products of enzymatic breakdown of an analyte are electrochemically detected. Enzyme immobilization on the electrode with maintained enzyme activity is a challenging task. The choice of immobilization method depends on many factors, such as the nature of the biological element, the type of transducer used, the physicochemical properties of the analyte and the operating conditions in which the biosensor should work, and overriding all these considerations is necessary for the biological element to exhibit maximum activity in its immobilized microenvironment. Generally, there are four regular methods for enzyme immobilization: adsorption, covalent bonding, crosslinking and entrapment (Nunes et al., 2006). The entrapment method is the most adapt for the realization of enzyme-based electrodes. This method refers to a mixture of biomaterial and monomer solution that polymerizes to a gel, trapping the biological component. Hydrogels are attractive materials in fabricating enzyme-based electrodes by entrapment method, since a hydrated gel provides an excellent matrix for encapsulation of functional enzymes (Pishko et al., 1991) that maintains intact the enzyme activity. Microneedles made by hydrogels are particularly attractive for making enzyme based electrodes for transdermal biosensing, because offers remarkable opportunities for moving microdevices from research laboratories to real field applications, and easy envisage to use point of care microdevices with pain free, minimally invasive, low cost and minimal training features, that are very attractive for both developed and emerging countries. Microneedles allow the realization of a new class of transdermal biosensors for electrochemical measurement of analytes of clinical interest, such as biomarkers, glucose, lactic acid, upon insertion of the needles in superficial layer of the skin. Diabetes is one of the leading causes of death and disability in the world. There is a large population suffering from this disease and the healthcare costs increase every year. It is a chronic disorder resulting from insulin deficiency and hyperglycemia and has a high risk of complications development for eyes, kidneys, peripheral nerves, heart and blood vessels. The lactic acid, or more commonly its negative ion called lactate, plays an important role in (sports) medicine, in the nutritional sector and touches environmental concerns. Determination of lactic acid concentration in blood is essential for the diagnosis of patient conditions in intensive care and during surgery. An elevated lactic acid level in blood is a major indicator of ischemic conditions of the respective tissue. This ischemic situation can be caused by all types of shock, suffocation and respiratory insufficiency, carbon monoxide or cyanide intoxication, heart failure, and so on.

Another reason for an altered lactic acid level is a disturbed lactic acid metabolism, which may be caused by diabetes or absorptive abnormalities of short chain fatty acids in the colon. In other fields of medicine, lactic acid plays an important role as well. In sports medicine (training of athletes or racing animals) or space medicine, blood lactic acid levels during exercise are indicators for training status and fitness. Quick diagnosis and early prevention are critical for the control of the disease status related to these two analytes. Most of devices that quantify glucose level operate by measuring it in blood sample that is generally taken from the fingertip since this procedure provides the most accurate result, but it also causes the patient pain because of fingertips contain many nerve endings. Moreover, the inability of current devices to continuously monitor the glucose level causes the need to do repetitive measurements each day resulting in protracted discomforts. Among the various conventional analytical methods available for the determination of lactic acid, colorimetric tests and chromatographic analysis are the most important. However, the major part of these methods is complex, laborious and slow, complicated by intensive sample pretreatment and reagent preparation. Therefore, the development of alternatives for glucose and lactic acid detection, with features of pain free, minimal invasion, biocompatibility, on one side, and simplicity, fast, low cost, real time with no need of sample preparation, on the other side, is very interesting and, above all, highly required from the dimensions of the market and huge demand.

Microfluidics is a multidisciplinary field of investigation, involving almost all the scientific branches of knowledge, such as physics, biology, engineering, chemistry and microtechnology. Conceptually, the idea under microfluidics is that fluids can be precisely manipulated using a microdevice built with technologies developed by semiconductor industry. Microfluidics can be defined as the science that studies the manipulation of small (10^{-9} to 10^{-18} litres) amounts of fluids, using channels with dimensions of tenths to hundreds micrometres. Microfluidic devices, commonly referred to as micro-TAS and LoC, have many advantages as they can decrease sample and reagent consumption and increase automation, thus minimizing the analysis time. Microfluidic devices exploit their most obvious characteristic, i.e. the small size, and less obvious characteristics of fluids in microchannels, such as laminar flow. The small dimension of devices allow for portability, so that biological and chemical samples can be tested on remote sites where there could not be access to traditional instrumentation. Microfluidic devices are nowadays employed in chemistry, biology, neuroscience, bioanalysis, biomechanics and other areas of biology and biomedical fields (Davis, 2008; Mehta et al., 2009). In the last ten years, the integration of mass transport

control into microfluidic devices by means of particular components, called membranes or more commonly filters, has showed a growing interest (De Jong et al., 2006). Filter science and technology is a broad and highly interdisciplinary field, where process engineering, material science and chemistry meet. Although the use of filters in microfluidics is spreading across many fields, most applications are found in analytical chemistry. Since analytical equipment is often sensitive to sample composition, in most cases samples cannot be directly analyzed and need a pretreatment. This may include selective removal of large components, impurities and dust on one side and low molecular weight components such as salts on the other. Furthermore, in many cases the concentration of the components of interest is below the detection limit of the analysis equipment. In such cases, removal of solvent is necessary. Filters can manage all these operations. Close to analytical applications, also new fields emerge in which filters are used, such as cell based studies, microreaction technology and fuel cells. Many different approaches were reported to realize microfluidic filters. A rough division into four fabrication methods can be made: direct incorporation of (commercial) filters, filter preparation as part of the device fabrication process, *in situ* preparation of filters and use of filter properties of bulk device material (De Jong et al., 2006). Currently, one of the most used is *in situ* preparation of the filter that starts with a microfluidic device and fabricates the filter inside it by polymerization of a photocurable hydrogel using UV light. The *in situ* photopolymerization allows creating the filter in any location of the microfluidic circuit without the need of a constriction region or other mechanisms that are commonly used to hold the beads. An additional benefit of this method is its application in existing chip formats, provided that the used chip material is transparent to UV light.

After this initial introduction, the PhD thesis is composed by other five chapters, from the second to the sixth: 1) materials and methods; 2) microneedles; 3) transdermal delivery of small molecules by microneedles based hybrid patch; 4) transdermal biosensing of biological molecules by microneedles based enzymatic electrodes; 5) filtration of small molecules by filter based microfluidic device.

The second chapter starts with a brief description of materials, hydrogels, SU-8 photoresist, PDMS, NOA and porous silicon, and fabrication processes, photolithography and soft imprint lithography, used. The description of the fabrication process, based on photographic reduction technique, of homemade plastic photomasks for fast prototyping of microfluidic devices is also reported. The chapter continues with the realization of microneedles based devices, such as hybrid device and enzymatic electrodes, and filter based microfluidic device using materials and fabrication processes previously described.

The third chapter is dedicated to the characterization of microneedles. In the first part, microneedles are characterized in terms of height and base, and curvature radius of the tips. In the second part, the indentation hardness, quantified by a penetration test, is characterized in order to verify the ability of microneedles to penetrate into skin.

A brief description of transdermal drug delivery by conventional approaches and the overcoming of their limits by using microneedles, topic already widely treated in this introduction, is summarized in the fourth chapter. The hybrid device based on microneedles, realized as described in the second chapter, is used for transdermal drug delivery. As proof-of-concept, the device is used for the releasing of fluorescein molecules, comparable to a small drug, into a buffer solution, that mimics the human interstitial fluid.

The fifth chapter treats briefly the novel trend on exploiting microneedles for transdermal biosensing of analytes of clinical interest, already widely described in this introduction. Microneedles based enzymatic electrodes, realized as described in the second chapter, for detection of glucose and lactic acid molecules are illustrated.

The sixth chapter summarizes the microfluidic filtration, a topic of relevant interest in many scientific fields, already widely discussed in this introduction. A small section is dedicated to the characterization of the homemade plastic photomask, realized as described in the second chapter. Microfluidic filter fabricated inside the microfluidic device for the filtration of small rhodamine molecules, realized as described in the second chapter, is characterized.

The thesis ends with conclusions, and some future perspectives.

2. Materials and Methods

Microfabrication, i.e. the generation of structures with dimensions in the range between tens of nanometers to millimeters, is essential in technology and modern science. It supports information technology and permeates society through its role in microelectronics, optoelectronics and so on. Microfabrication has its foundations in microelectronics and it will continue to be the basis for microprocessors, MEMS, flexible electronic devices, biomedical systems in the foreseeable future. Photolithography is the most successful process in microfabrication. It is used to pattern parts of a thin film using the UV light. Essentially, almost all devices with dimensions in the range between 100 nm to millimeters are manufactured by this process. Microfabrication is also shifting towards areas outside microelectronics, such as biotechnology and biochemistry (Bhansali et al., 2012). Materials science gives great support to development of innovative application of microfabrication: traditional materials are defined as hard materials, since the most used one is the semiconductor silicon, but in some of these fields, there is the need to use a set of materials, the so-called soft materials, much more larger than the classic one, which comprises polymers, hydrogels and also biological matter. A high number of new microfabrication processes, the soft lithography processes, has been demonstrated for fabricating high quality structures with sizes ranging from 30 nm to hundreds of micrometers (Rogers et al., 2005; Qin et al., 2010). One of the most famous processes is the soft imprint lithography that consists in transferring a pattern from a soft structure to an imprint material.

This chapter is divided in two parts: the first part is dedicated to the description of microfabrication processes, photolithography and soft imprint lithography, together with soft and hard materials used, in particular hydrogels, SU-8 photoresist, PDMS, NOA and porous silicon; in the second part, these microfabrication processes and materials are illustrated in practical realization of some devices, such as hybrid device and enzymatic electrodes based on microneedles, and microfluidic device based on filter.

2.1. Materials

Materials traditionally used in microfabrication are silicon, and silicon related materials such as silicon nitrides and oxides, porous silicon, amorphous silicon and so on, but also metals (gold, aluminum, platinum, nickel, chromium), glasses of many different kind. In photolithography, some particular light sensitive commercial polymers, note as photoresists, are commonly exploited. Most of them are expensive and primarily limit the use in some applications, like *in vivo* application, due to the bio-incompatibility. In order to overcome

these limitations, there is the need of alternative materials, such as soft materials. In the following, hard and soft materials are described in details.

2.1.1. Hydrogels

Hydrogels are polymeric networks able to swell and/or retain aqueous solutions. Hydrogels are attractive materials in fabrication of biodevices, since a hydrated gel provides an excellent matrix for encapsulation of functional biological molecules, such as enzymes and peptides. Main advantages of hydrogels are briefly summarized in the following: 1) micropatterning by photolithography; 2) development of biocompatible tissue/sensor interface; 3) near-physiological conditions that minimize protein denaturation helping them to carry out their full biological functions; 4) three-dimensional geometry enables them to contain large quantity of sensing reagent, thereby increasing their signal-to-noise ratio and sensitivity. Hydrogels are divides in two types: natural, like alginates, chitosan and synthetic, as poly(ethylene glycol) diacrylate (or PEGDA), polyacrylamide and so on. One of the most widely used is the PEGDA, available commercially from Sigma Aldrich. PEGDA is a hydrophilic and biocompatible hydrogel that has been suggested for use in a variety of biomedical applications (Oh, 2009). PEGDA is poorly immunogenic, non-toxic, is readily cleared by the kidneys and is approved by the Food and Drug Administration for internal consumption. Moreover, it is an elastic material. PEGDA is commercially available over a wide range of molecular weights (M_n) from low, that means polymer with tight mesh, to high values, that means polymer with wide mesh. PEGDA with high M_n is useful in applications that require an hard material, such as the realization of microneedles for skin penetration, instead PEGDA with low M_n is adapt in those cases that need of a robust material but not so hard, like a microfluidic filter for the separation of biological samples. The key chemical constituent of the PEGDA is showed in Figure 2.1.

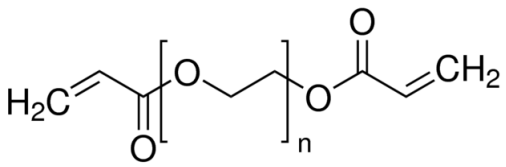

Figure 2.1 Chemical composition of the PEGDA with molecular weight M_n.

The terminal acrylates groups, in presence of a photoinitiator and exposed to UV light, allow the hydrogel to be crosslinked at room temperature, in order to form an insoluble hydrogel network. Photoinitiators most frequently used are 2-hydroxy-2-methyl-1-phenyl-propan-1-one

or known as darocur 1173 (see Figure 2.2 (A)) and 2-hydroxy-2-methylpropiophenone (see Figure 2.2 (B)), available commercially from BASF and Sigma Aldrich, respectively.

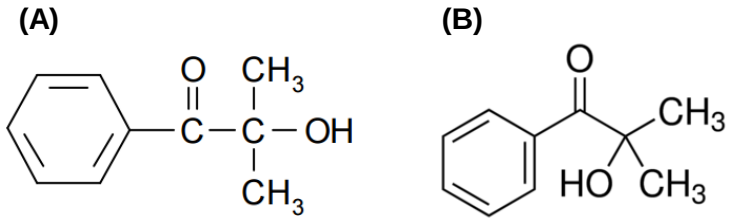

Figure 2.2 Chemical composition of 2-hydroxy-2-methyl-1-phenyl-propan-1-one (A) and 2-hydroxy-2-methylpropiophenone (B).

2.1.2. SU-8 photoresist

SU-8 (see Figure 2.3) is an epoxy based high contrast photoresist, designed for micromachining and other microelectronic applications, where a thick, chemically and thermally stable image is desired.

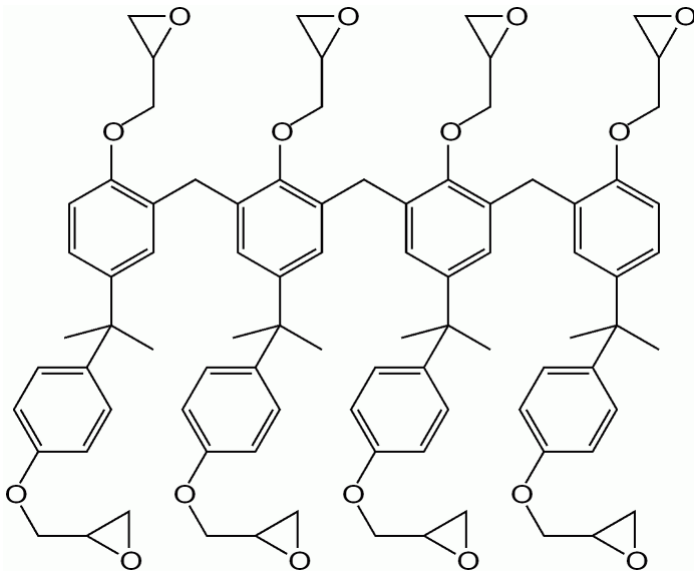

Figure 2.3 Chemical composition of the main constituent in SU-8 photoepoxy: eight oligomers are available for a high degree of crosslinking upon photoexposure.

SU-8 is available commercially from MicroChem in different viscosities, thus enabling a wide range of thicknesses (0.5 to 650 μm with a single coat process) that can be obtained (MicroChem). SU-8 photoresist has excellent imaging characteristics and is able of producing very high aspect ratio structures. SU-8 is a negative photoresist, therefore is best suited for applications where it is casted, cured and left permanently on the device, like in the fabrication of a microfluidic device.

2.1.3. Polydimethylsiloxane

PDMS is available commercially from several companies, but the most famous is the silicone elastomer kit from Dow Corning called Sylgard 184. It contains a base and a curing agent that, once mixed, polymerize to form PDMS (Ottosen, 1999). The key chemical constituents of the PDMS are two and they are showed in Figure 2.4.

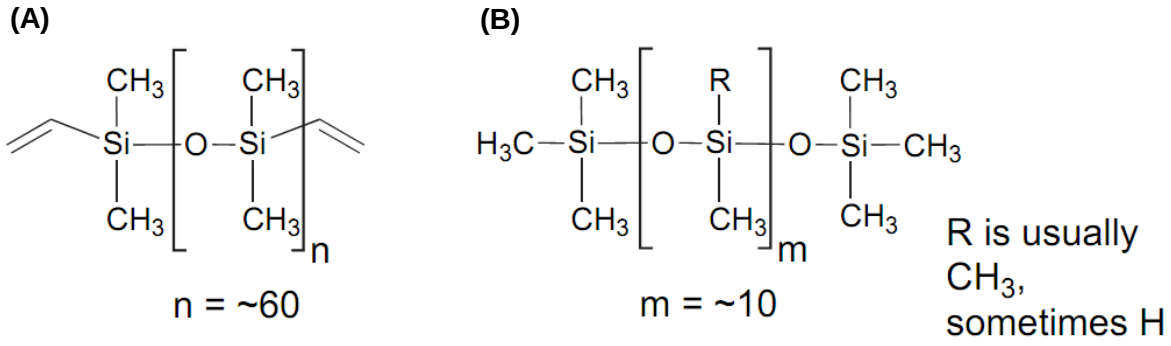

Figure 2.4 Key PDMS pre-cursors, where (A) is a vinyl-terminated siloxane oligomer and (B) is a shorter, partially hydrosilane-terminated siloxane oligomer. The base contains (A) and a platinum complex, whereas the curing agent contains (A) and (B). Each methyl-hydrosiloxane oligomer contains a minimum of three hydrosilane (Si-H) groups available as hydrosilation reaction sites.

Both components of the kit contain siloxane oligomers terminated with vinyl groups (see Figure 2.4 (A)). The curing agent also includes cross-linking siloxane oligomers (see Figure 2.4 (B)), which each contains at least three silicon-hydride bonds (Si-H). The base includes a platinum-based catalyst that cures the elastomer by an organometallic cross-linking reaction. When the base and the curing agent are mixed together, hydrosilation takes place between the vinyl ($SiCH=CH_2$) and hydrosilane (SiH) groups of the copolymer pre-cursors, forming Si-CH_2-CH_2-Si linkages. The hydrosilane groups provide multiple reaction sites, giving rise to three-dimensional cross-linking. One advantage of this type of reaction is that no waste products are generated. Increased temperature will accelerate the cross-linking reaction. Changing the curing agent-to-base ratio alters the properties of the resulting cured elastomer: as the ratio of curing agent-to-base increases, more rigid elastomer results. A ratio of 1:10 guarantees a good trade-off between flexibility and rigidity. The properties of PDMS are surprisingly close to those could be obtained from glass and plastic. It is flexible and reversibly deformable. Many of the properties (optical, electrical, mechanical) exhibited by PDMS are very desirable for fabricating microfluidic devices (McDonald et al., 2002).

2.1.4. Norland optical adhesive

NOA is a single component liquid adhesive, available commercially from Norland Products, that cures in seconds to an hard polymer when exposed to UV light (Norland Products). NOA is sensitive to the UV light with a wavelength range from 320 to 380 nm, with peak sensitivity around 365 nm. The outstanding characteristic of this adhesive is its extremely fast cure. To fully cure the material requires 2 J/cm^2 of energy. NOA cures to a hard film, but it will not become brittle. NOA cures not before the desired time. It is also extremely stable when not exposed to UV light. It has a small amount of resiliency that provides strain relief from vibrations or temperature extremes. This toughness insures long term performance of the adhesive bond. NOA cures from the surface down and longer cures are required for thicker films to allow UV light to penetrate to the full depth. This adhesion improves with age, with optimum adhesion reached after room temperature aging for one week. This optimum adhesion can be accelerated by aging at 50 °C for 12 hours. The cured adhesive can withstand temperatures from -150 °C to 125 °C. Many of the properties (optical, mechanical, etc) exhibited by NOA are very desirable for fabricating microfluidic devices.

2.1.5. Porous silicon

Porous silicon can be simply described as a network of air holes in a silicon matrix. In most cases, the porous silicon structure is formed by electrochemical dissolution of a doped crystalline silicon wafer in hydrofluoric acid (HF) based solution (Smith et al., 1992). In the anodic I-V curve of silicon in HF based solution, showed in Figure 2.5, it's possible to distinguish three regions, called A, B, C.

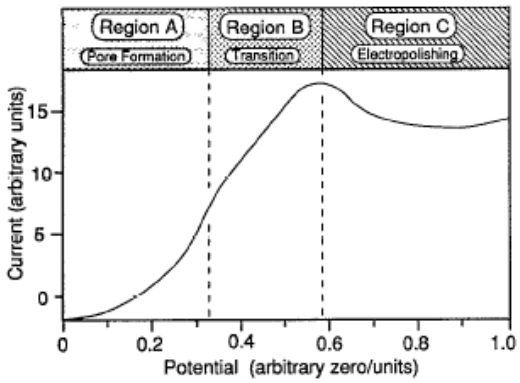

Figure 2.5 Regions of pore formation (A), transition between pore formation and silicon electropolishing (B) and silicon electropolishing (C).

Pore formation takes place in region A. At anodic overpotentials in excess of the current peak, region C, silicon electropolishes. At intermediate overpotentials, region B, a transition zone

exists where pore formation and electropolishing compete for control over the surface morphology. The resulting structure within the region B is generally porous in nature, but the pore diameters increase rapidly as the electropolishing potential is approached. Porous silicon shows a great variety of morphologies dependent on the doping type and level of the silicon substrate and the electrochemical etching parameters. Usually for a given substrate and electrolyte, only one type of pore structure can be obtained. The International Union of Pure and Applied Chemistry guidelines define ranges of pore sizes that exhibit characteristic absorption properties: pores characterized by a diameter $\leq$ 2 nm define microporous silicon; for sizes in the range 2-50 nm the porous silicon is mesoporous; pores diameters > 50 nm are typical of macroporous silicon. The porous silicon is an ideal material as optical biosensor transducer and it allows the label-free detection (Dhanekar et al., 2013). Its principal advantages are: 1) low-cost material and fabrication process; 2) large specific surface area (~ 500 m^2/cm^3); 3) rapidly and effectively interaction with chemical species; 4) evident changes in several physical properties usable for label-free sensing (reflectivity, photoluminescence, electrical conductivity, optical waveguiding, etc); 5) easy integration in hybrid systems (MEMS, LoC, etc); 6) compatibility with microelectronic technologies; 7) chemically modification of its surface possible to enhance selectivity in analyte detection. The label-free sensing mechanism used is based on the change of the porous silicon refractive index on exposure to the substances to be detected, due to their infiltration into the pores; the consequence of the refractive index variation is a change in the reflectivity/transmittivity spectrum of the photonic structure. Photonic structures as porous silicon resonant photonic structures as Fabry-Perot interferometers, Bragg reflectors, optical microcavities, are realized exploiting intensively multilayer fabrication capability (Sailor, 2012). This is possible because the porous silicon fabrication process is self-stopping; an as etched porous silicon layer is depleted of holes and any further etching only occurs at the pores tips. The refractive index modulation of a porous silicon multilayered structure can be realized by alternating different proper currents densities during the electrochemical etching of crystalline silicon.

2.2. Microfabrication processes

Microfabrication processes, like photolithography and soft imprint lithography, allow the patterning of a material. Although the photolithography is the most used, the soft imprint lithography is gaining consensus in some fields like biology and chemistry. In the following, these two microfabrication processes are described.

2.2.1. Photolithography

Photolithography is a standard process in microfabrication for transferring a geometrical pattern from a photomask to a photoresist deposited on a substrate. The process sequence, illustrated in Figure 2.6 and described in details in literature (Sze, 2008), can be summarized in the following steps:

1) spin coat: the photoresist is spin coated onto the substrate to the desired thickness;
2) soft bake: the photoresist is warmed on a hotplate to evaporate the solvent;
3) exposure: the photoresist is exposed to UV light with a quartz/chrome photomask by a mask aligner in hard, soft or flood (that is without photomask) contact mode;
4) post exposure bake: the photoresist is again warmed on a hotplate to harden the exposed or unexposed regions depending on the photoresist type, negative or positive respectively;
5) development: a solvent is used to dissolve unexposed or exposed regions (depends on the photoresist type, negative or positive respectively), leaving a relief structure of photoresist on the substrate.

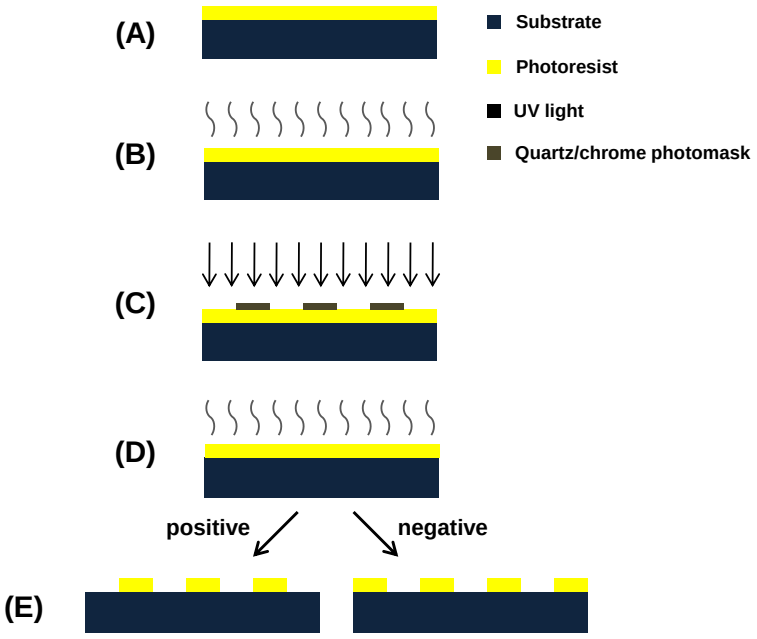

Figure 2.6 Schematic of the photolithographic process sequence for structuring a layer of photoresist (not to scale): (A) spin coat; (B) soft bake; (C) exposure; (D) post exposure bake; (E) development.

Some devices illustrated in the next paragraphs are realized using the photolithographic process, with eventual small modifications.

2.2.2. Soft imprint lithography

In order to fabricate NOA device containing microfluidic channels, the soft imprint lithography process is used. It consists to transfer a pattern from a soft structure to an imprint material. This process can be divided mainly in two parts:

1) fabrication of the PDMS stamp by soft lithography replica molding process;
2) fabrication of the device in NOA from the PDMS stamp.

As well described by many texts (Qin et al., 2010), the steps to fabricate a stamp in PDMS by soft lithography replica molding can be summarized as (see Figure 2.7 (A)-(C)):

1) the SU-8 mould is fabricated by patterning SU-8 photoresist, with desired thickness, on a silicon substrate using photolithography (all parameters, like soft bake time, exposure time and so on are reported in details on the SU-8 datasheet (MicroChem));
2) the SU-8 mould is silanized exposing it to trimethylchlorosilane (TMCS) vapours for 20 minutes in order to facilitate the future removal of the PDMS stamp from the SU-8 mould;
3) to form the PDMS, one part of curing agent and ten parts of base (by volume) are mixed rather carefully;
4) the mixture, full of air bubbles, is degassed under vacuum for 30 minutes or more;
5) the PDMS is dispensed onto SU-8 mould avoiding to trap air;
6) the SU-8 mould with the PDMS above is cured through heating at 80 °C for 1 hour;
7) the PDMS stamp is peel off from the SU-8 mould.

The process for producing a microfluidic device in NOA, described in details in this text (Bartolo et al., 2008), is illustrated in Figure 2.7 (D)-(H). It is can be sketched in the following points:

1) the opposite of the PDMS stamp, called PDMS anti-stamp, is fabricated from the PDMS stamp;
2) the PDMS anti-stamp is put in contact with a flat PDMS and the empty space between them is filled with NOA;
3) all this is exposed to UV light for 10 s at 40 mW/cm^2 without photomask in order to partially polymerize the NOA;
4) the PDMS anti-stamp is removed, the remainder part is pressed against a glass slide and exposed to UV light for 10 minutes at 40 mW/cm^2 without photomask in order to complete the polymerization of the NOA;
5) the flat PDMS is removed.

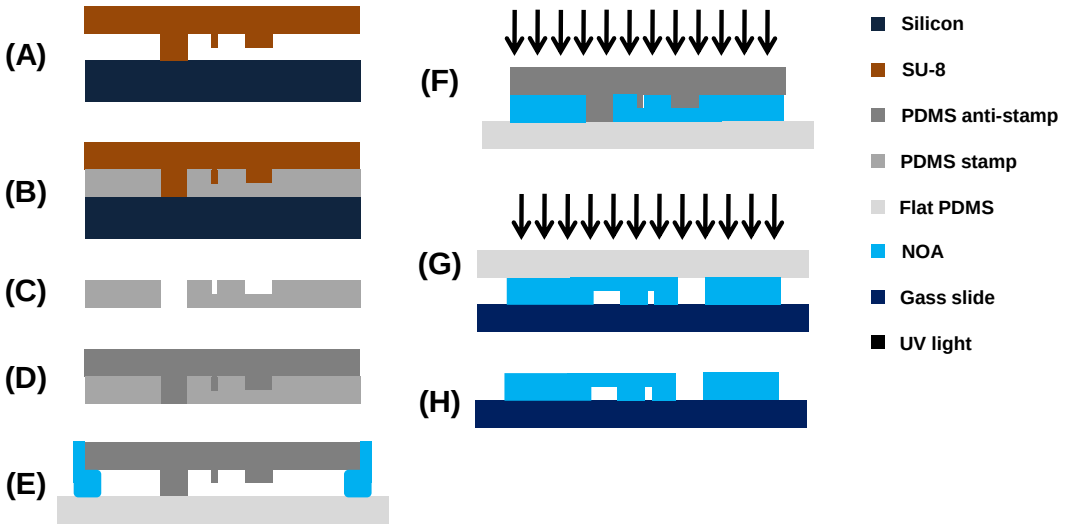

Figure 2.7 Scheme process to fabricate a microfluidic device in NOA by soft imprint lithography (not to scale): (A) fabrication of the SU-8 mould using photolithography; (B) fabrication of the PDMS stamp; (C) PDMS stamp after peeling; (D) fabrication of the PDMS anti-stamp; (E) filling the space between PDMS anti-stamp and flat PDMS with NOA; (F) exposure to UV light without photomask; (G) removing of the PDMS anti-stamp and exposure to UV light without photomask; (H) removing of the flat PDMS.

2.3. Microneedles fabrication

Microneedles are three-dimensional structures and represent key components of some biomedical devices, often acting as an interface between the device and the patient's body. Due to well-established microelectronic fabrication technologies, silicon, and silicon related materials, such as silicon nitrides and silicon oxide, is one of the most used for making microneedles. On the other hand, silicon is fragile and definitely not a biocompatible material, since it can cause local inflammations or silicosis, so that even in low invasive devices it could result unhealthy. As alternative materials, polymers can be used to overcome intrinsic limitations of silicon, like PDMS, PEGDA and so on. PEGDA is particularly attractive for this aim because rapidly hardens at room temperature in presence of a photoinitiator on exposure to UV light, so that it is possible to fabricate microneedles by photolithographic process.

Microneedles are made with a hydrogel, obtained mixing PEGDA 250 (M_n=250) and darocur 1173 at 2% volume/volume (v/v), that behaves as a negative photoresist. The main steps of the process for producing a microneedle array by photolithography, as illustrated in Figure 2.8 (A)-(F), are:

1) the quantity of 1 ml of negative photoresist is deposited on a quartz slide by drop casting technique and then it is hardened by exposure to UV light for 10 s without

photomask, obtaining about 1 mm thick layer that is the flexible support for the following microneedle array;

2) a silicone vessel is fulfilled with the negative photoresist;
3) the hardened layer of photoresist on the quartz slide is overturned and putted on the silicone vessel to close it;
4) the hardened layer of photoresist on the quartz slide is exposed to UV light with a quartz/chrome photomask, containing circles with a specific diameter, in soft contact mode to the quartz slide;
5) all this is developed in deionized water for 2 minutes, in order to remove the unpolymerized photoresist, and is dried with nitrogen;
6) the quartz slide is separated from the hardened layer of photoresist by means of tweezers, obtaining a flexible microneedle array.

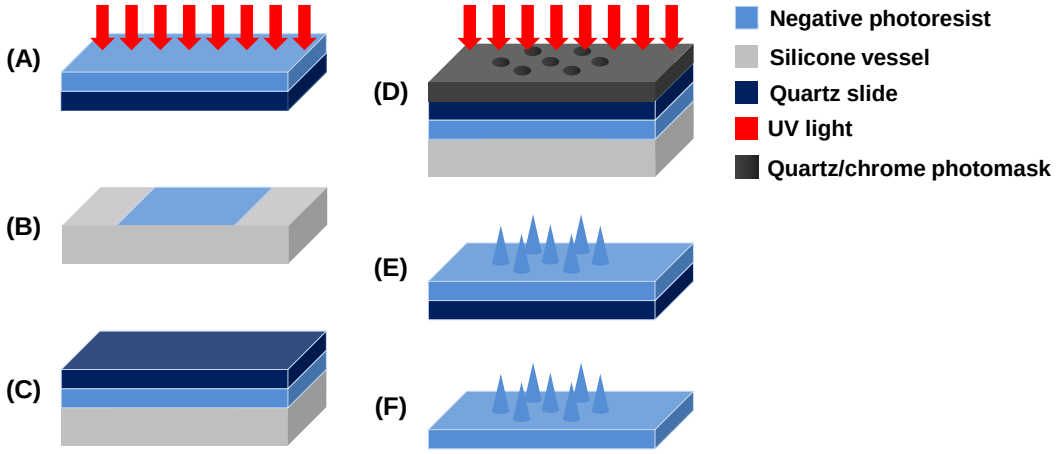

Figure 2.8 Flow chart of the fabrication process of the microneedle array (not to scale): (A) formation of the photoresist layer; (B) filling of the silicone vessel with photoresist; (C) direct contact between the hardened layer of photoresist and the photoresist contained inside the vessel; (D) exposure to UV light with a quartz/chrome photomask; (E) development in deionized water; (F) separation between the quartz slide and the hardened layer of photoresist.

Soft and post exposure bakes are not required, because this photoresist does not contain any solvent to be evaporate and should not be hardened by heating.

2.4. Microneedles based hybrid device fabrication

Microneedles promise innovative and breakthrough applications in biomedicine, both in diagnostics and therapeutics. The development of microneedles has been driven in the first by finding a painless alternative to hypodermic injections, and interesting devices based on microneedles are currently progressing through clinical trials for delivery of molecules and vaccines, such as insulin, parathyroid hormone and influenza vaccine. More extended

functions have been imagined since it became clear that microneedles were the almost perfect interface between the derma and any medical device for theranostic. As a matter of fact, microneedles permit exchanges between outside of the human body and the interstitial fluid under the stratum corneum of the skin, that normally is impermeable to all molecules with molecular weight larger than 500 Da like antibodies and proteins. In order to produce a proof-of-concept device for transdermal drug delivery, whose operation will be described in the chapter 4, porous silicon and microneedle array are combined together.

Porous silicon structures can be optically encoded, which means that they can exhibit specific photonic signatures. Photonic structure based on free-standing porous silicon membrane is fabricated by electrochemical etching of p^{++} crystalline silicon (0.001 Ωcm resistivity, <100> oriented, 500 µm thick) in HF (50% in volume), deionized water, and ethanol solution (1:1:1), in dark and at room temperature. Before anodization dissolution, silicon substrate is immersed in HF solution for two minutes in order to remove native oxide layer. Time breaks of 5 s are used during etching process in order to recover HF concentration at dissolution edge and start next layer formation with zero current density: in this way, density current is always the same for each layer. At the end of the porous multilayer formation, the anodization current density is quickly increased up to 600 mA/cm^2 for 3 s and then to 800 mA/cm^2 for 5 s, in order to turn the reaction into the electrochemical polishing state and separate the porous silicon membrane from the silicon substrate. The etching area is 0.98 cm^2. Porous silicon membrane is oxidized into absolute ethanol solution for 24 hours at room temperature, in order to make it hydrophilic. From the optical point of view, the porous silicon membrane behaves as a Bragg mirror. It is a periodic structure made alternating layers of low (n_L) and high (n_H) refractive index, or high (P_H) and low (P_L) porosity, respectively, whose thicknesses (d_L and d_H) satisfy the relation $2(n_H d_H + n_L d_L) = m\lambda_B$, where m is the order of the Bragg condition. The layer stack is usually denoted as $[n_L n_H]^N$, where N is the number of periods. The Bragg mirror is made by 30 periods. High porosity layers are obtained applying a current density of 200 mA/cm^2 for 0.6 s (n_L=1.60, d_L=78.03 nm); low porosity layers are obtained applying a current density of 100 mA/cm^2 for 0.87 s (n_H=1.92, d_H=65.04 nm). Porosities and thicknesses are estimated by spectroscopic ellipsometry measurements (data not showed here). Values of refractive index are calculated at λ=500 nm by using a Bruggeman approximation (Aspnes et al., 1979).

Microneedle array is realized as described in the paragraph 2.3, with these parameters: UV light intensity of 18 mW/cm^2, exposure time of 7.5 s and base's diameter of 400 µm.

The hybrid device is fabricated by assembling the porous silicon membrane, that acts as drugs/molecules reservoir, and the polymeric microneedle array, that allows the release of drugs/molecules, as showed in Figure 2.9.

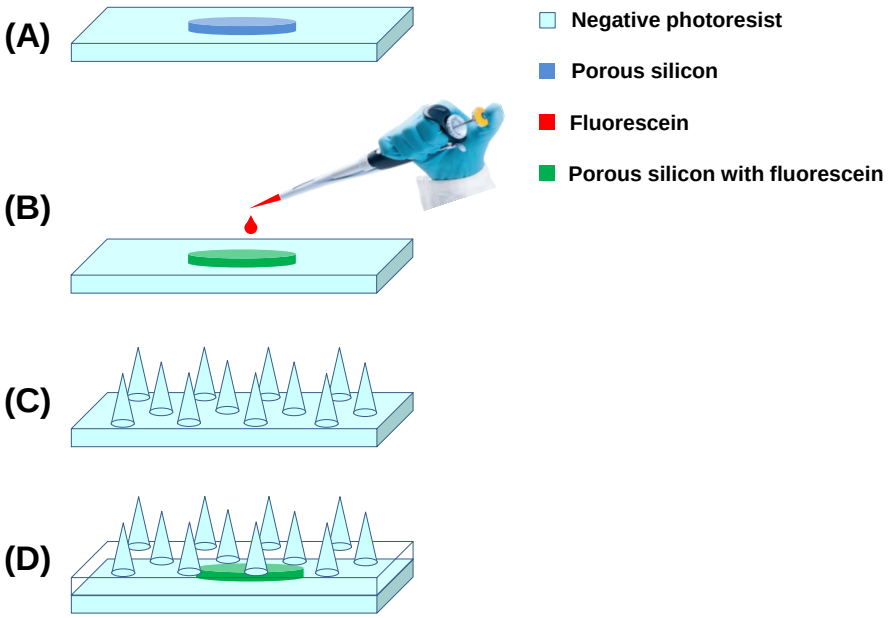

Figure 2.9 Schematic of the assembling of the hybrid device (not to scale): (A) fabrication and placing of the porous silicon membrane on the hardened layer of negative photoresist; (B) loading of the porous silicon membrane with fluorescein; (C) microneedle array fabrication; (D) assembling between the hardened layer of photoresist and the microneedle array.

The porous silicon oxidized membrane is fabricated and placed on the hardened layer of negative photoresist (see Figure 2.9 (A)) and then is loaded with 50 µl of saturated aqueous solution of fluorescein by drop casting technique (see Figure 2.9 (B)). The porous silicon membrane is blocked and sealed by bonding the microneedle array (see Figure 2.9 (C)) to the layer of negative photoresist: drops of negative photoresist are poured around the porous silicon membrane and exposed to UV light at 18 mW/cm^2 for 10 s without photomask (see Figure 2.9 (D)). The negative photoresist is equal to that used in the paragraph 2.3 for fabricating the microneedles.

2.5. Microneedles based enzymatic electrodes fabrication

Transdermal biosensing by microneedles offers remarkable opportunities for moving biosensing technologies from research labs to real field applications, allowing realizing microdevices with many advantages like painless, minimal training. Microneedles allow realizing a novel class of transdermal biosensors for electrochemical measurement of analytes of interest for public health, like glucose and lactic acid. These electrochemical biosensors are called microneedles based enzymatic electrodes. In order to produce proof-of-concept devices

for transdermal biosensing, whose operations will be described in the chapter 5, two microneedles based enzymatic electrodes have been realized, one for the detection of glucose and the other for the lactic acid.

The two microneedles based enzymatic electrodes are fabricated by means of photolithography and sputter deposition. Microneedles based enzymatic electrodes are constituted by gold-coated microneedle arrays. The fabrication process is equal for both electrodes, therefore it is discussed only that used for making electrode for the detection of glucose. The microneedle array is realized in way similar to that described in the paragraph 2.3, with these parameters: UV light intensity of 18 mW/cm^2, exposure time of 25 s and base's diameter of 400 µm. The negative photoresist, called negative photoresist 1, used in the first step of that process for making the flexible support is made by adding 2% v/v of darocur and 1% w/v of the redox mediator, vinylferrocene, to PEGDA. The vinylferrocene increases the conductivity of PEGDA. The negative photoresist, called negative photoresist 2, used to filling the silicone vessel, and therefore to make microneedles, is made by adding glucose oxidase enzyme (GOx) in phosphate buffered saline (PBS) (pH 6.0) at 20 mg/mL concentration to 90% v/v of photoresist 1. In order to electrically contact the microneedle array, as showed in Figure 2.10, a 160 nm thick layer of gold is deposited on the back of the flexible support (see Figure 2.10 (A)).

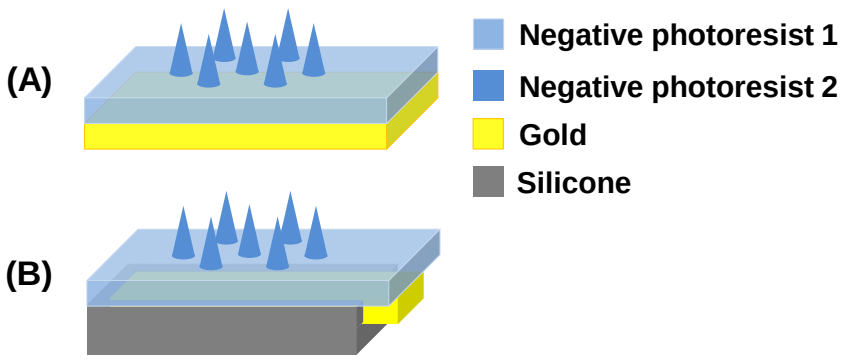

Figure 2.10 Flow chart of the fabrication process of the electrical contact of the microneedle array (not to scale): (A) gold deposition on the back of the microneedle array; (B) partial waterproofing of the gold layer by hardened liquid silicone rubber.

The deposition is made by sputtering, at room temperature with a current of 30 mA and a deposition time of 240 s. The gold layer is partially covered by a thin layer of commercial liquid silicone rubber, hardened at room temperature in 2 hours (see Figure 2.10 (B)). The silicon rubber film on the back of the gold layer prevents direct contact between the electrode and the electrolytic solution during the electrochemical characterizations. As showed in Figure 2.10 (B), a small area of the gold layer remained uncovered by silicone, in order to

allow the electric contact with the electrochemical setup. However, the uncovered gold is not immersed into the electrolytic solution, in the course of electrochemical measurements. The electrode for the electrochemical detection of lactic acid is realized in the same way of that for the detection of glucose, but using lactate oxidase enzyme (LOx) in PBS (pH 6.5) at 15 mg/mL concentration instead of GOx.

2.6. Filter based microfluidic device fabrication

In order to fabricate the filter inside the microfluidic device made in NOA, whose operation will be described in chapter 6, a photomask has to be used. Usually, the photomasks, made in quartz/chrome, are very expensive due to the complicated fabrication process and the use of expensive instrumentation. In the following, it is described a cheap and practical homemade process to make photomask on photographic film by photographic reduction technique (see Figure 2.11), which are particularly suitable for the fast prototyping of microfluidic devices:

1) designing of the reverse patterns to those to transfer to the photomask by a Computer Aided Design (CAD) software;
2) scaled print (typically 10:1) of the mask patterns onto paper sheet using an office printer;
3) mask patterns photographic reduction (typically 10 times) and transferring from paper onto photographic negative film by an enlarger used in reduction mode;
4) chemical treatment of the photographic negative film, in order to obtain the plastic photomask in which there is the reverse of designed patterns.

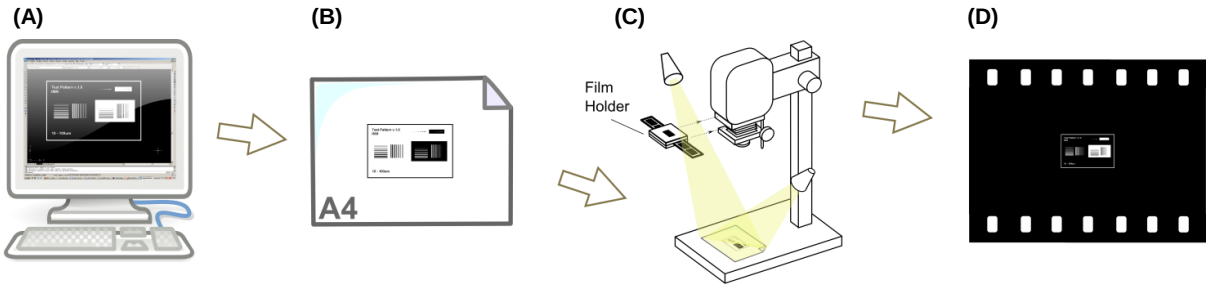

Figure 2.11 Scheme process to realize a plastic photomask by the photographic reduction technique (not to scale): (A) CAD design of photomask patterns; (B) scaled print of the photomask patterns on a paper sheet; (C) photomask patterns optical reduction and transferring from paper to photographic film; (D) chemical treatment of the plastic photomask.

Filter is fabricated inside the microfluidic device by *in situ* photopolymerization. The material used to make the filter is a hydrogel obtained by mixing the 50% v/v of PEGDA 575 (M_n=575), the 5% v/v of the photoinitiator 2-hydroxy-2-methylpropiophenone and the 45%

v/v of deionized water. This material behaves as a negative photoresist. Since this material is completely transparent and it can be hardly seen in the microchannels, 2 μL of fluospheres carboxylate yellow-green (1 μm diameter) are added for imaging purposes. In this way the filter, made by exposing this fluorescent solution to UV light, would be observable in fluorescence imaging, and thus it could be characterized by a microscope used in fluorescence mode. The circuit, constituted by two channels, is filled by this negative photoresist and only a specific area is exposed to UV light for 1 s at 40 mW/cm^2 with the plastic photomask in soft contact mode. For the exposure, it is used a mask aligner, but others standard UV exposure systems, like a microscope coupled with a UV lamp or a microscope coupled to a Digital Micromirror Device (DMD) and a UV lamp, can be used. The homemade plastic photomask contains a transparent line, whose dimensions are equals to those of the filter. Then, the circuit is flushed with deionized water for several minutes in order to remove the unpolymerized photoresist, obtaining the filter inside the microfluidic device. Soft and post exposure bakes are not required, since this photoresist does not contain any solvent to be evaporate and should not be hardened by heating.

3. Microneedles

Microneedles are key components of some biomedical devices, in consideration of they provide an interface between the device and the body of a patient for extracting, sampling or releasing fluidic substances (Mukerjee et al., 2004; Valdés-Ramírez et al., 2012; Liu et al., 2013). The concept of microneedles was proposed in the 1970s, but it was not realized experimentally until the 1990s, when the industry of microelectronics provided the tools essential to make such small structures. After the first microneedle arrays reported in the literature (Campbell et al., 1991), a lot of papers were published on the fabrication of microneedles by using several fabrication methods and materials (Ashraf et al., 2011). Various fabrication methods were developed and used for microneedles fabrication like hot embossing, laser micromachining, micromolding, coherent porous silicon etching, photolithography. Nowadays, the photolithography process is widely used in industrial fields for manufacturing of microdevices such as microprocessors and MEMS. It is simple, does not require complicated instrumentation and is adapt for the industrial manufacturing that is on large scale, therefore it is the most suitable process for the fabrication of the microneedles. Material selection is very important to design and fabricate microneedles for any particular application. Many researchers used silicon for microneedles fabrication, because it is abundant, inexpensive, highly pure and processing is amenable to miniaturization. On the other hand, silicon is a brittle material and can be harmful to health. As alternative materials, polymers can be used to overcome intrinsic limitations of silicon, such as PDMS and PEGDA. PEGDA is particularly attractive for this aim because rapidly hardens at room temperature in presence of a photoinitiator on exposure to UV light, so that it is possible to fabricate microneedles by photolithographic process.

In this chapter the microneedle array, fabricated as described in paragraph 2.3, is characterized. In particular, in the first part microneedles are characterized in terms of height and base, and curvature radius of the tips. In the second part is proved that the microneedles are adapted for skin penetration, measuring the indentation hardness and performing a penetration test.

3.1. Height, base and curvature radius characteristics

Some digital images (see Figure 3.1 (A)-(B)) and optical photographs (see Figure 3.1 (C)-(D)) of the microneedle array, made in PEGDA and darocur by photolithographic process, described in the paragraph 2.3, are reported in Figure 3.1.

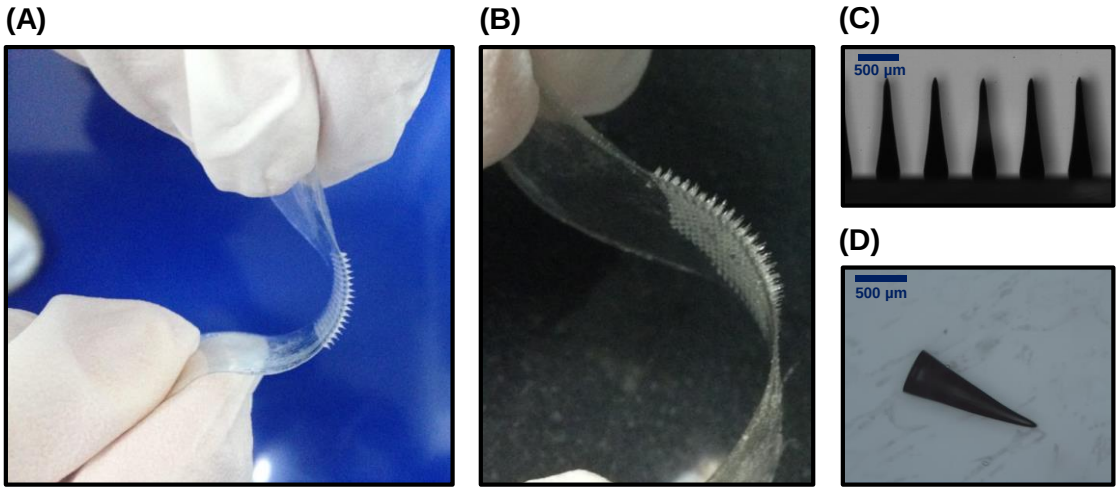

Figure 3.1 Digital ((A)-(B)) and optical ((C)-(D)) images of the microneedle array based on negative photoresist, made of PEGDA and darocur.

It is possible to see that the adhesion of the microneedle array on the photoresist layer is perfect and the structure can be deformed by fingers without breaking or damaging the microneedles.

Results of the characterization of several microneedle array fabricated in this way are showed in Table 3.1, Table 3.2 and Table 3.3.

Microneedle array	Exposure time (s)	Photomask array	Height (µm)
A1	5	A	1340±20
A2	7.5	A	1430±25
A3	10	A	1600±18
A4	12.5	A	1700±21
A5	15	A	2240±19

Table 3.1 Height of the microneedles with a light intensity of 18 mW/cm^2 and array A.

Microneedle array	Exposure time (s)	Photomask array	Height (µm)
B1	5	B	1230±15
B2	7.5	B	1430±11
B3	10	B	1500±13
B4	12.5	B	1700±10
B5	15	B	2000±12

Table 3.2 Height of the microneedles with a light intensity of 18 mW/cm^2 and array B.

Microneedle array	UV light intensity (mW/cm^2)	Photomask array	Height (µm)	Curvature radius (µm)
C1	9	B	210±7	11.3±0.3
C2	9	A	940±8	9.0±0.2
C3	12	A	1180±15	10.8±0.2
C4	15	A	1380±12	7.8±0.3
C5	18	A	1450±10	2.0±0.1

Table 3.3 Height of the microneedles and curvature radius of the tips of these microneedles with an exposure time of 7.5 s and array A, B.

The quartz/chrome photomask used for the exposure to UV light in the photolithographic process contains two arrays of transparent circles, as it can be seen in Figure 3.2 (A): arrays A and B (see Figure 3.2 (B)), where the diameters of circles are 400 µm and 250 µm, respectively.

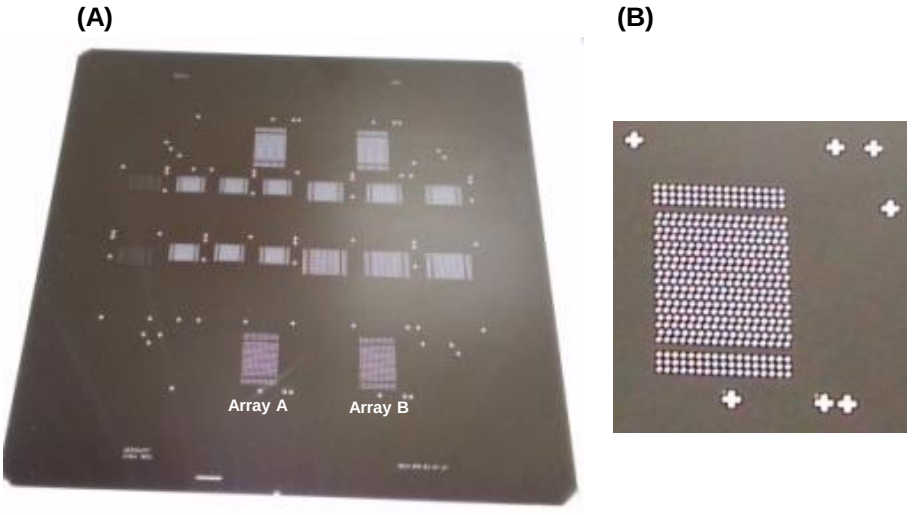

Figure 3.2 (A) Quartz/chrome photomask; (B) array B.

Table 3.1 and Table 3.2 show the heights of the microneedles at fixed UV light intensity (18 mW/cm^2 for both) and array (A and B, respectively): the height grows on increasing the time of exposure to UV light. Table 3.3 shows the height of the microneedles and the curvature radius of the tips of the microneedles at fixed exposure time (7.5 s for both) and array (A and B): the height grows on increasing of the UV light intensity and the curvature radius is less than 15 µm therefore microneedles are adapt for skin penetration (Davis et al., 2004).

3.2. Indentation hardness and skin penetration properties

The effective penetration of microneedles into the skin is a major issue, because microneedles can broke due to uneven skin surface or human error during the penetration. Microneedles insertion studies were typically performed in biological tissue, but this can present some disadvantages, in that tissue samples are often heterogeneous, unstable and difficult to obtain. In addition, the use of biological materials sometimes presents legal issues. Thus, it is desirable to overcome these limitations by using an artificial material in place of skin. The indentation hardness property of microneedles is compared with that of a commercial polymeric film layer, parafilm M, used as artificial skin very similar to the surface layer of the pig skin (Larrañeta et al., 2014). The indentation hardness is measured by means of force/distance spectroscopy tool of the atomic force microscope (AFM). The force/distance spectroscopy tool supports the acquisition of force vs distance curve, which is the plot of the force, between the AFM tip and the tip of a microneedle or the parafilm M layer, as function of their relative distance. The force spectroscopy plots show a greater slope, and thus a greater indentation hardness, of the tip of the microneedle (see Figure 3.3 (A)) compared to that of the parafilm M layer (see Figure 3.3 (B)).

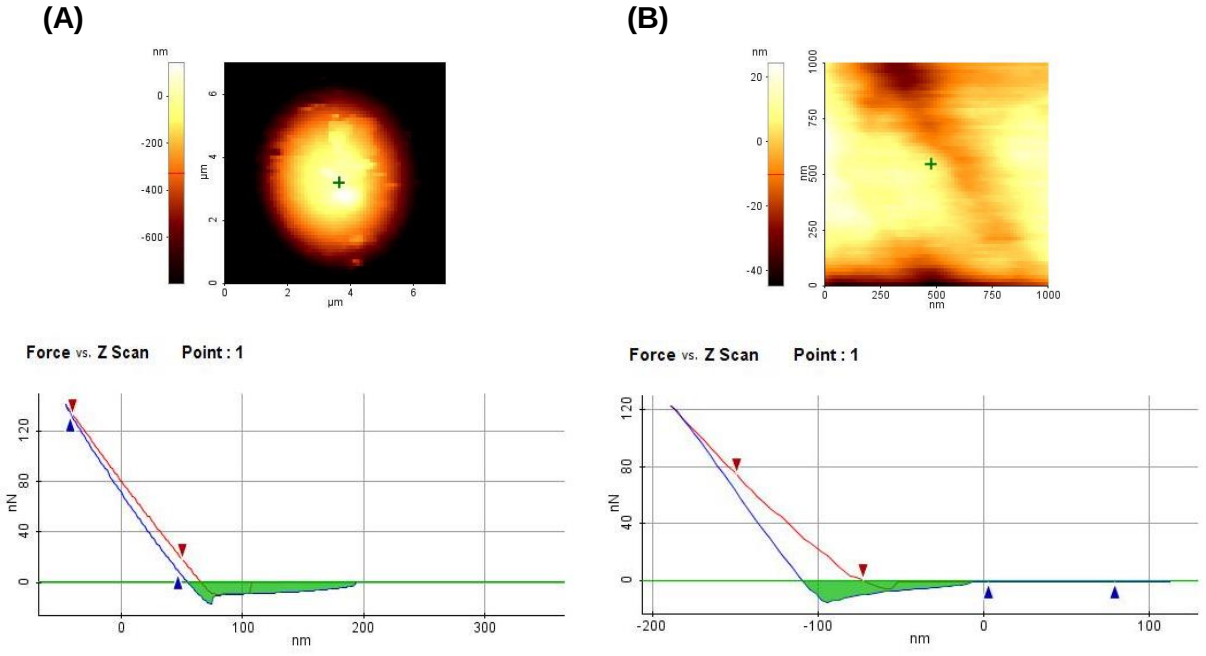

Figure 3.3 AFM relative indentation hardness measurements of the tip of a microneedle (A) and of a parafilm M layer (B).

This result is essential in quantify the possibility of microneedles in tissue penetration.

In order to prove the effective insertion of microneedles into the skin, penetration test was performed by using eight parafilm M layers folded on themselves, that mimics the pig skin (Larrañeta et al., 2014). Figure 3.4 shows tilted (A), lateral (B) and top (C) views of the reversed first layer, once separated from the others.

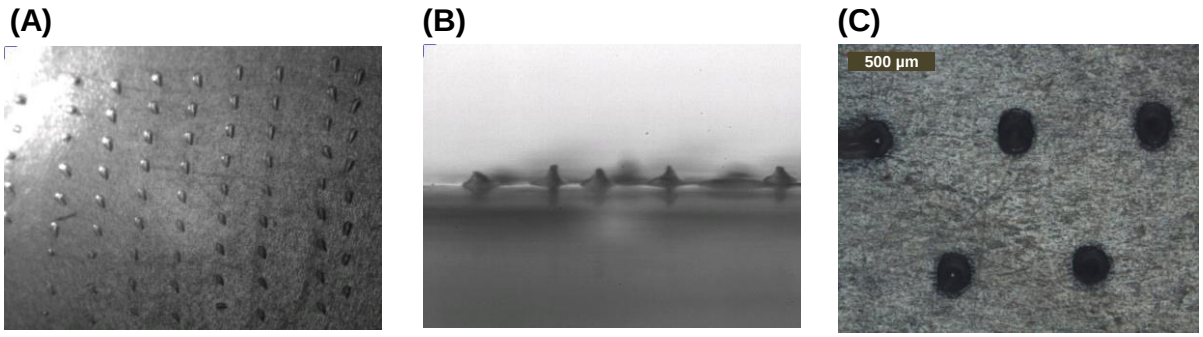

Figure 3.4 Tilted (A), lateral (B) and top (C) views of the first parafilm M layer after reversing.

It is clear that the microneedles penetrate the first layer and impress their shape, molding the surface.

In Figure 3.5, top views of firsts five layers of the artificial skin are showed.

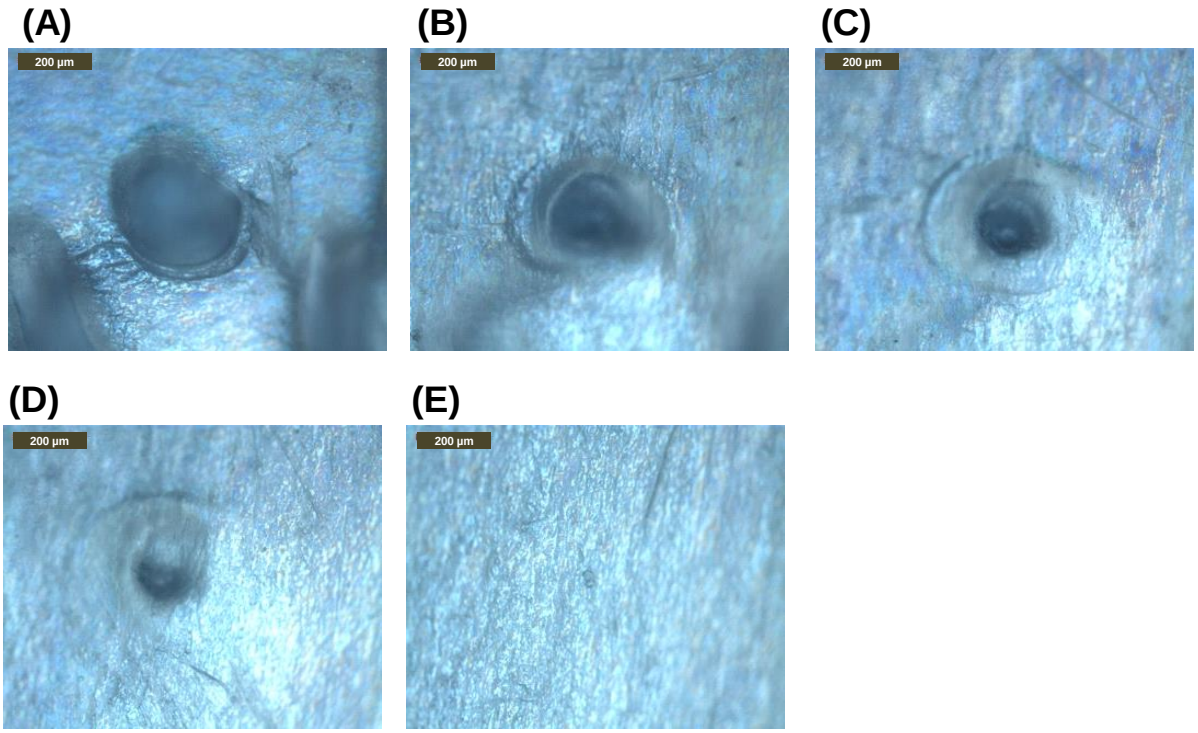

Figure 3.5 Optical microscope images of the first (A), the second (B), the third (C), the fourth (D) and the fifth (E) parafilm M layer after microneedles penetration.

In particular, Figures 3.5 (A)-(E) show the holes that the same microneedles were performed on first, second, third, fourth and fifth layer. Since each parafilm M layer is 160 µm thick,

microneedles penetrate the first four layers for a total distance of 640 µm, proving a good penetration strength.

4. Transdermal delivery of small molecules by microneedles based hybrid patch

When oral administration of drugs is not feasible due to poor drug absorption or enzymatic degradation in the gastrointestinal tract or liver, injection using a painful hypodermic needle is the most common alternative. An approach that is more appealing to patients, and offers the possibility of controlled release over time, is drug delivery across the skin using a patch (Touitoi, 2002). However, transdermal delivery is severely limited by the inability of the large majority of drugs to cross skin at therapeutic rates due to the great barrier imposed by skin's outer stratum corneum layer. To increase skin permeability, a number of different approaches has been studied, ranging from chemical/lipid enhancers (Cevc, 2004; Williams et al., 2012) to electric fields employing iontophoresis and electroporation (Denet et al., 2004; Kalia et al., 2004) to pressure waves generated by ultrasound or photoacoustic effects (Doukas et al., 2004; Mitragotri et al., 2004). Although the mechanisms are all different, these methods share the common goal to disrupt stratum corneum structure in order to create holes big enough for molecules to pass through. The size of disruptions generated by each of these methods is believed to be of nanometer dimensions, which is large enough to permit transport of small drugs and, in some cases, macromolecules, but probably small enough to prevent causing damage of clinical significance. An alternative approach involves creating larger transport pathways of microns dimensions using arrays of microneedles. These pathways are orders of magnitude bigger than molecular dimensions and, therefore, should readily permit transport of macromolecules, as well as possibly supramolecular complexes and microparticles. Despite their very large size relative to drug dimensions, on a clinical length scale they remain small. Although safety studies need to be performed, it is proposed that microscale holes in the skin are likely to be safe, given that they are smaller than holes made by hypodermic needles or minor skin abrasions encountered in daily life.

In this chapter the hybrid device based on porous silicon and polymeric microneedle array, fabricated as described in the paragraph 2.4, is proposed as a proof-of-concept device for transdermal drug delivery. In particular, the device operation is described and experimental proved using it for the releasing of fluorescein molecules into a buffer solution.

4.1. Microneedles based hybrid patch

Hybrids device (see Figure 4.1 (A)) and patch (see Figure 4.1 (B)) based on microneedle array and free-standing porous silicon membrane are fabricated as described in the paragraph 2.4.

Figure 4.1 Hybrids device (A) and patch (B).

The hybrid device includes a porous silicon free-standing membrane with a Bragg mirror optical structure which reflects a specific bright color in the visible. Figure 4.2 shows the scanning electron microscope (SEM) images of the free-standing membrane (A), made alternating layers of low and high porosity, and the morphology of one of those two layers (B), constituted of mesopores.

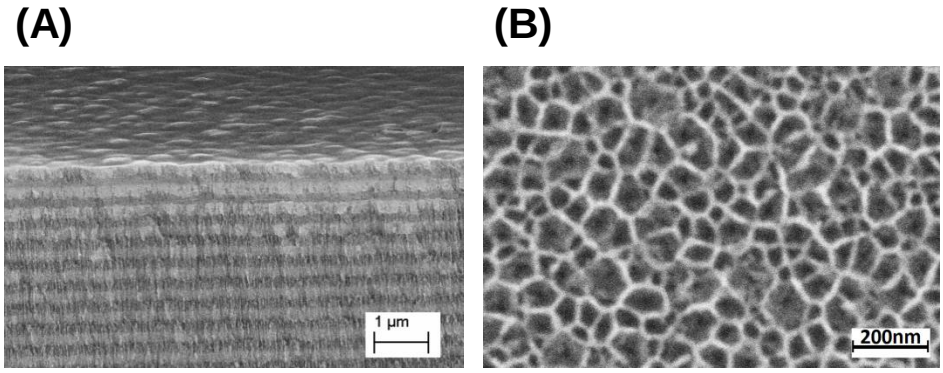

Figure 4.2 SEM images of the cross-section of the free-standing porous silicon membrane (A) and of the surface of the porous silicon layer (B).

4.2. Optically monitored administration of fluorescein molecules

A sketch of the device operation is showed in Figure 4.3, where the porous silicon membrane, that acts as drugs/molecules reservoir, is firstly loaded with the drug (see Figure 4.3 (A)), then the drug diffuses into the polymeric matrix of the microneedles (see Figure 4.3 (B)) and, finally, the drug is released into the external solution (see Figure 4.3 (C)). As a proof of concept, a dye molecule, 332 Da fluorescein, and PBS solution 1X at pH 7.2 are used as drug and external solution. PBS mimics the human interstitial fluid.

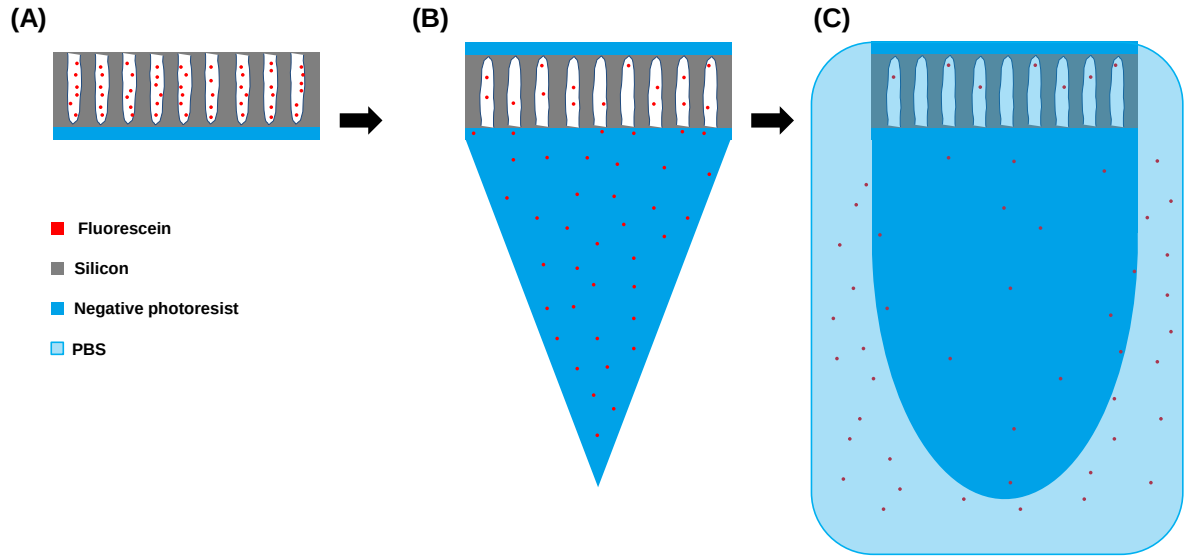

Figure 4.3 (A) Loading of the porous silicon membrane with the fluorescein molecules; (B) diffusion of the fluorescein molecules into the nanoporous polymeric matrix of the microneedles; (C) releasing of the fluorescein molecules into the PBS solution due to the swelling of microneedles. All images are not to scale.

Fluorescent images reported in Figure 4.4 experimentally confirm the diffusion of the fluorescein molecules from the porous silicon membrane into the polymeric matrix of the microneedles.

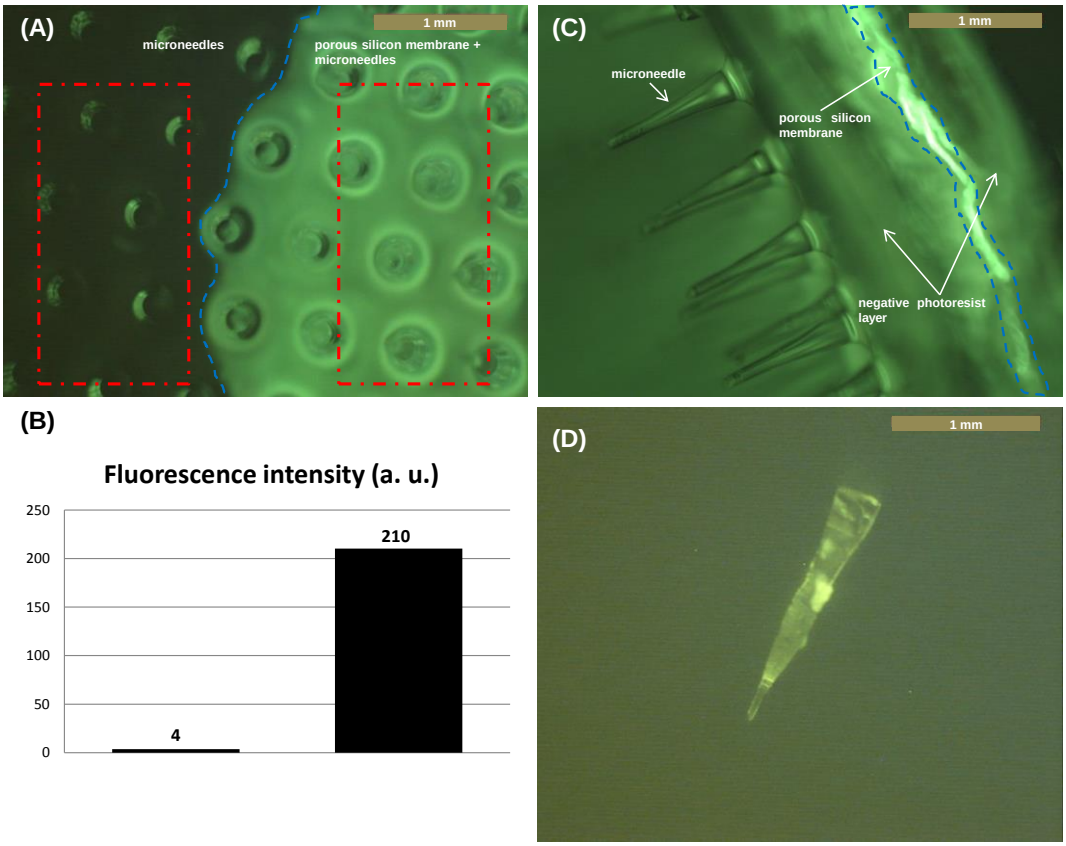

Figure 4.4 (A) Top view of the device acquired in fluorescence mode: the blue line underlines the profile of the porous silicon membrane placed under the microneedles (right side) compared to the only microneedles (left

side); (B) fluorescence intensities of the areas inside the red rectangles of (A); (C) lateral view of the device acquired in fluorescence mode: the blue line underlines the profile of the porous silicon membrane placed under the microneedles; (D) single microneedle detached from the device after fluorescein loading.

The migration of the luminescent molecules from porous silicon membrane to microneedles starts just after the bonding of device constituents and spontaneously occurs also in absence of the external solution. Top view of the device, acquired in fluorescence mode, is showed in Figure 4.4 (A): the blue line shows the porous silicon membrane placed under the microneedles and the only microneedles. Only the area of microneedle array overlapping the porous silicon membrane is fluorescent. A quantitative estimation, by counting the fluorescence intensities of the areas inside the red rectangles (see Figure 4.4 (B)), reveals an high intensity (210 counts) for the porous silicon membrane just under the microneedle array (see right side of the Figure 4.4 (A)) and a low intensity (4 counts) for only microneedles outside the area of the porous silicon membrane (see left side of the Figure 4.4 (A)), also proving that polymeric microneedles do not show intrinsic fluorescence signal. Cross section of the whole device (see Figure 4.4 (C)) and picture of a single microneedle (see Figure 4.4 (D)), detached from the negative photoresist layer, have been acquired in fluorescence mode. Both images show that the fluorescein is almost uniformly distributed from the base to the tip of the microneedles: this result proves that the fluorescein molecules are not chemically bonded neither mechanically fixed into the polymeric matrix and can easily diffuse from the mesoporous of the membrane to the nanoporous polymeric matrix (Li et al., 2013). The diffusion naturally stops when equilibrium between the fluorescein concentration into the porous silicon membrane and the rest of the device is reached.

The porous silicon membrane has a double function: it acts as a drugs/molecules reservoir, and, since its color changes depending on what fills its pores, it can be used to optically monitor the drugs/molecules loaded and released from it. In Figure 4.5 (A), the reflectivity spectra of the porous silicon membrane after oxidation, fluorescein loading and PBS immersion after 2 hours are showed. The Bragg multilayer, i.e. a stack of alternating films with proper thicknesses and refractive indexes which satisfy the Bragg relationship, is an interferometric mirror that exhibits maximum reflection for a specific interval of wavelengths, the so called stop band. The stop band shifts if thicknesses or refractive indexes are modified: is this the case of porous silicon based Bragg mirror, where the stop band position depends on the porosity of the stack. When the porous silicon membrane is filled by molecules, the optical spectrum red shifts towards higher wavelengths, since the material appears denser on average: in case of fluorescein loading more than 100 nm of shift can be measured (see Figure

4.5 (A)). The new position of the resonant wavelength is stable: the diffusion of fluorescein in the polymeric matrix does not modify the optical spectrum, i.e. there is not a relevant depletion of the porous silicon membrane. On the contrary, a strong blue shift (more than 50 nm) of the spectra after immersion in PBS for 2 hours proves the release of fluorescein from the porous silicon membrane to the microneedles. The shifts of the optical spectrum correspond to changes in color of the device from violet to green and then to blue, which can be clearly monitored by naked eye, as showed in Figure 4.5 (B).

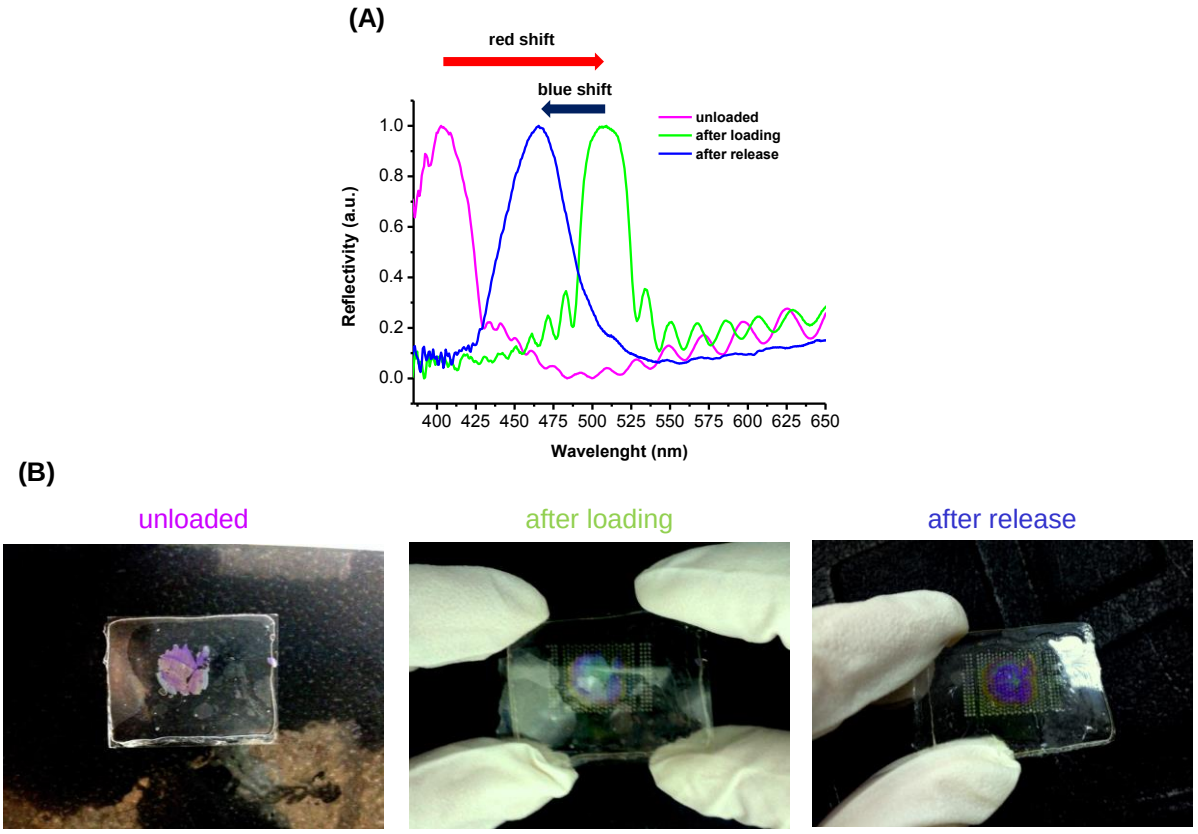

Figure 4.5 Spectroscopic reflectometry (A) and naked eye (B) characterizations after oxidation, fluorescein loading and release of fluorescein in the PBS solution.

In Table 1, the spectroscopic reflectometry data relative to the absolute position of the wavelength peak and the blue shift of Bragg optical structure peak are reported as function of immersion time in PBS (0, 2, 4, 8 and 24 hours).

	Before PBS	After 2h in PBS	After 4h in PBS	After 8h in PBS	After 24h in PBS
Peak position	508.2±0.3	450.5±0.4	444.9±0.5	445.6±0.9	436.6±0.2
Blue shift	-	57.7±0.1	63.3±0.1	62.7±0.2	71.6±0.1

Table 4.1 Spectroscopic reflectometry data of absolute position and shift of Bragg optical structure peak as function of immersion time in PBS solution.

The fluorescence intensity as function of immersion time in PBS (0, 2, 4, 8 and 24 hours) of the microneedle array (see Figure 4.6) is strictly related to the blue shift of the porous silicon membrane optical spectrum: as a matter of fact, the blue shift indicates a depletion of the porous silicon tank, to which corresponds a decrease of the fluorescence intensity of the microneedles as the immersion time in PBS increases. The decreasing of the fluorescence intensity means that fluorescein molecules diffuse from the microneedles to the PBS solution. It is verified that the fluorescence decrease is not due to a decay of the radiative properties of the molecules by measuring the fluorescence intensity of loaded microneedles not exposed to PBS solution as a function of time, as reported in Figure 4.6.

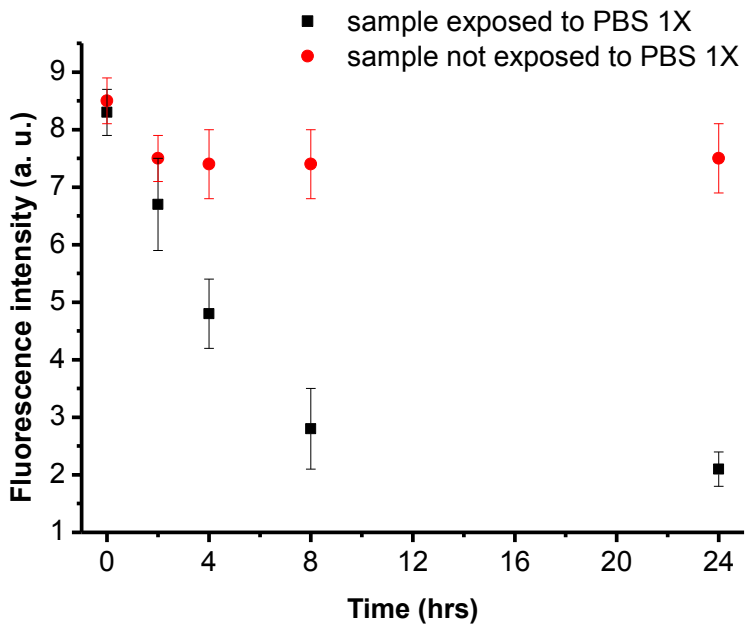

Figure 4.6 Changing of the fluorescence intensity of microneedles of two devices, one immersed in the PBS solution and the other no, as function of time.

After the equilibrium is reached, the fluorescent signal does not change in time, so it is possible to attribute the strong emission change of the device exposed to PBS solution to a real dispersion of fluorescein in the external solution.

In order to confirm that the decreasing of microneedles fluorescence intensity is due to the release of fluorescein in the PBS solution, those data are compared with those reported in ref. (Donnelly et al., 2012) as showed in Figure 4.7.

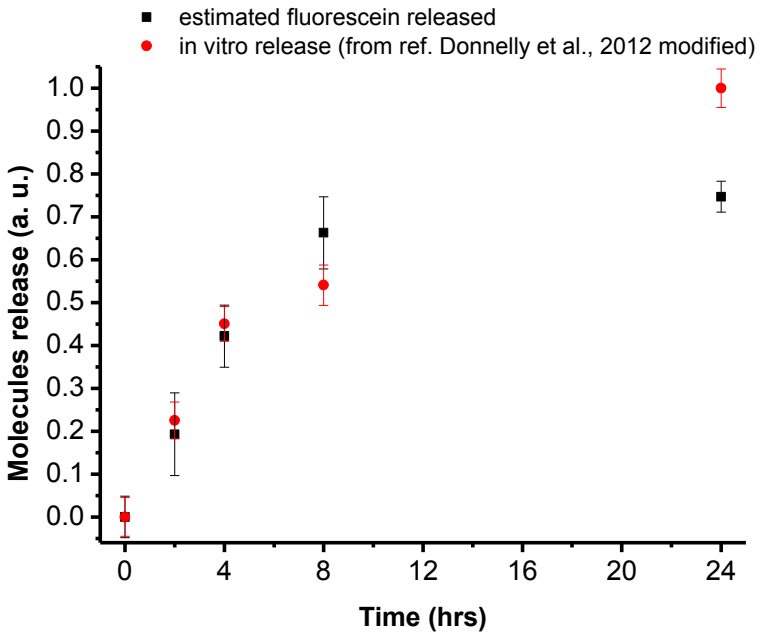

Figure 4.7 Comparison between the estimated fluorescein released in PBS and data of *in vitro* release as reported in ref. (Donnelly et al., 2012).

Methylene blue (320 Da) loaded in hydrogel-forming microneedles patch, made of 15% w/w poly(methylvinylether/maelic acid) and 7.5% w/w poly(ethyleneglycol), was released and quantified *in vitro* experiment (Donnelly et al., 2012). If it was assumed that the estimated fluorescein was proportional to the complement of the fluorescence intensity, i.e. molecules released were estimated as *1-Ifn* (where *Ifn* is the fluorescence intensity normalized to its maximum value), the comparison with respect to data reported in ref. (Donnelly et al., 2012) highlighted a really similar behavior, and the kinetic of the release was also very similar.

5. Transdermal biosensing of biological molecules by microneedles based enzymatic electrodes

A growing general attention on public health, in particular on nutrition and sport activity, indicated as primary prevention of diseases, such as obesity and diabetes as well as cancer, supported a continuous development of diagnostic devices in the last ten years. Currently, the most important physiological parameters is measured in laboratories and requires dedicate instrumentation, not available for self-diagnostic at home. Electrochemical biosensors, and in particular microneedles based enzymatic electrodes, offer an unique opportunity to realize point of care microdevices with pain free, minimally invasive, low cost and minimal training features (Ventrelli et al., 2015). The immobilization of the enzyme on the electrode with maintained enzyme activity is the most hard task for the realization of the device. The immobilization method influences the performances, the response time, the sensitivity, the stability and the lifetime of the biosensor. The enzyme immobilizing method should promote a rapid propagation of generated electrons and avoid nonspecific binding and electrode failing. Electrode features can be optimized by using several matrices in which enzymes can be dispersed. Among many available from material science studies, hydrogels are excellent enzyme encapsulation materials, that avoid enzymatic binding, allow analyte molecules diffusion and interaction with the enzymes, provide near physiologic conditions and avoid enzymes denaturation (Yan et al., 2010). PEGDA rapidly hardens at room temperature in presence of a photoinitiator on exposure to UV light, therefore it gives an excellent encapsulation of the enzyme. Moreover, this peculiarity can be used to fabricate microneedles by photolithographic process.

In this chapter two microneedles based enzymatic electrodes, realized as described in the parahraph 2.5, are proposed as proof-of concept devices for transdermal biosensing. In particular, the operation of the two devices is described and experimental proved for the electrochemical detection of glucose and lactic acid molecules.

5.1. Microneedles based enzymatic electrodes

The enzymatic electrode for the detection of glucose, fabricated as described in the paragraph 2.5, is showed in the Figure 5.1.

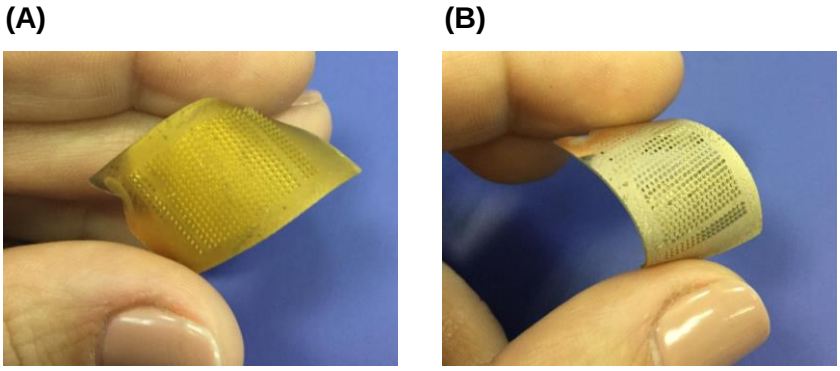

Figure 5.1 Pictures front (A) and back (B) of the microneedles based enzymatic electrode for the detection of glucose.

The device is completely flexible, in particular the microneedle array (see Figure 5.1 (A)) could be deformed without breaking, and the back is continuously covered by gold (see Figure 5.1 (B)), assuring a good electrical contact. The length of the microneedles is of about 500 µm. The enzymatic electrode for the detection of lactic acid is equal to this, therefore it is not showed.

5.2. Electrochemical detection of glucose and lactic acid molecules

A scheme of the device working principle and of the experimental setup geometry is illustrated in Figure 5.2.

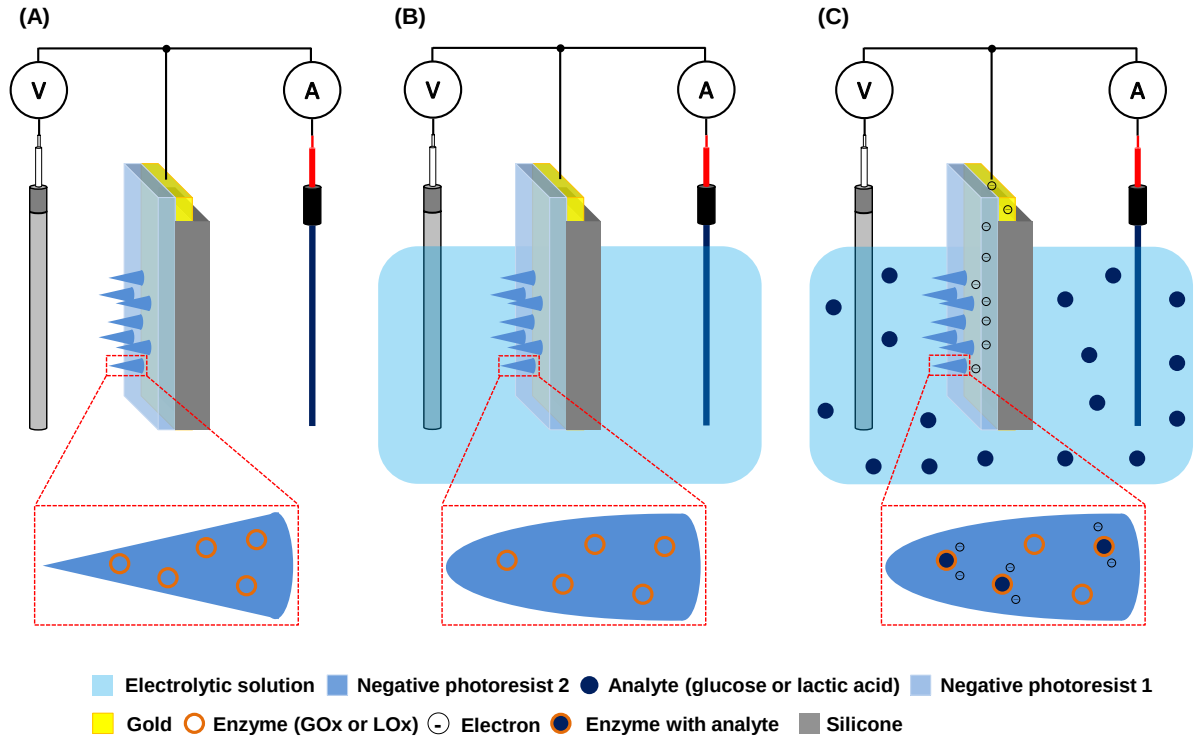

Figure 5.2 (A) Sketch of the three electrode cell; (B) immersion of the three electrodes inside the electrolytic solution, with following swelling of the microneedles; (C) penetration of the analyte molecules (glucose or lactic

acid) inside the microneedles and redox interaction between the enzyme (GOx or LOx) and the analyte (glucose or lactic acid), with following generation of electrons. All images are not to scale.

The setup is constituted of a three electrode cell (see Figure 5.2 (A)): a platinum wire is the auxiliary electrode, a saturated silver chloride (silver/silver chloride 3 M) is the reference electrode and the microneedles based enzymatic electrode (that for glucose or that for lactic acid) is the working electrode. The three electrodes are immersed in an electrolytic solution (see Figure 5.2 (B)), that mimics the interstitial fluid, made of PBS at 10 mM concentration (pH 7.4) mixed with 0.48 mM magnesium chloride ($MgCl_2$), deoxygenated with nitrogen during the electrochemical measurements. The swelling of the polymeric matrix of the microneedles allow to analyte molecules (glucose or lactic acid) to penetrate into the microneedles and to interact with the enzyme (GOx or LOx) locked inside the porous matrix (see Figure 5.2 (C)), resulting in the generation of electrons collected by auxiliary electrode.
Sensing mechanism is based on redox reactions between analyte (glucose or lactic acid) and enzyme (GOx or LOx), summarized in equations (1)-(3) in case of glucose and equations (4)-(6) in case of lactic acid: through these reactions, the analyte concentration is transduced into an electrical current value (Heller et al., 2008; Wang, 2008). In particular, the biocatalytic reaction involves reduction of enzyme flavin group (FAD) in its reduced form ($FADH_2$), reported in equation (1) for glucose and equation (4) for lactic acid. Glucose is oxidized to D-glucono-1,5-lactone (equation (1)) and lactic acid is oxidized to pyruvic acid (equation (4)). An artificial mediator, the vinylferrocene, promotes the electrons charge transfer between FAD center and enzymatic electrode surface (equations (2) and (5) for glucose and lactic acid, respectively): $\text{vinylferrocene}_{ox}$ and $\text{vinylferrocene}_{red}$ are the oxidized and reduced forms of the mediator. The reduced form of the mediator is then re-oxidized on the electrode, giving a current signal (proportional to the glucose or lactic acid concentration) while regenerating the oxidized form of the mediator (equation (3) for glucose and equation (6) for lactic acid).

$$\beta - D - glucose + GOx(FAD) \rightarrow D - glucono - 1{,}5 - lactone + GOx(FADH_2) \quad (\mathbf{1})$$

$$GOx(FADH_2) + 2vinylferrocene_{ox} \rightarrow GOx(FAD) + 2vinylferrocene_{red} + 2H^+ \quad (\mathbf{2})$$

$$2vinylferrocene_{red} \rightarrow 2vinylferrocene_{ox} + 2e^- \quad (\mathbf{3})$$

$$L - lactic\ acid + LOx(FAD) \rightarrow pyruvic\ acid + LOx(FADH_2) \quad (\mathbf{4})$$

$$LOx(FADH_2) + 2vinylferrocene_{ox} \rightarrow LOx(FAD) + 2vinylferrocene_{red} + 2H^+ \quad (\mathbf{5})$$

$$2vinylferrocene_{red} \rightarrow 2vinylferrocene_{ox} + 2e^- \quad (\mathbf{6})$$

5. Transdermal biosensing of biological molecules by microneedles based enzymatic electrodes

Cyclic voltammetry technique is used to characterize the activity of the redox mediator vinylferrocene, in presence of the enzyme (GOx or LOx) incorporated into the polymeric matrix. During the cyclic voltammetry measurements, the potential applied between the working electrode and the reference electrode is linearly changed and the current between the working electrode and the auxiliary electrode is measured. For working electrode containing GOx, the potential has varied from -100 to 700 mV, and backward, with scan rates 30, 50, 70 and 100 mV/s (see Figure 5.3 (A)). For working electrode containing LOx, the potential has varied from -100 to 600 mV, and backward, with scan rates 30, 50, 70 and 100 mV/s (see Figure 5.3 (B)).

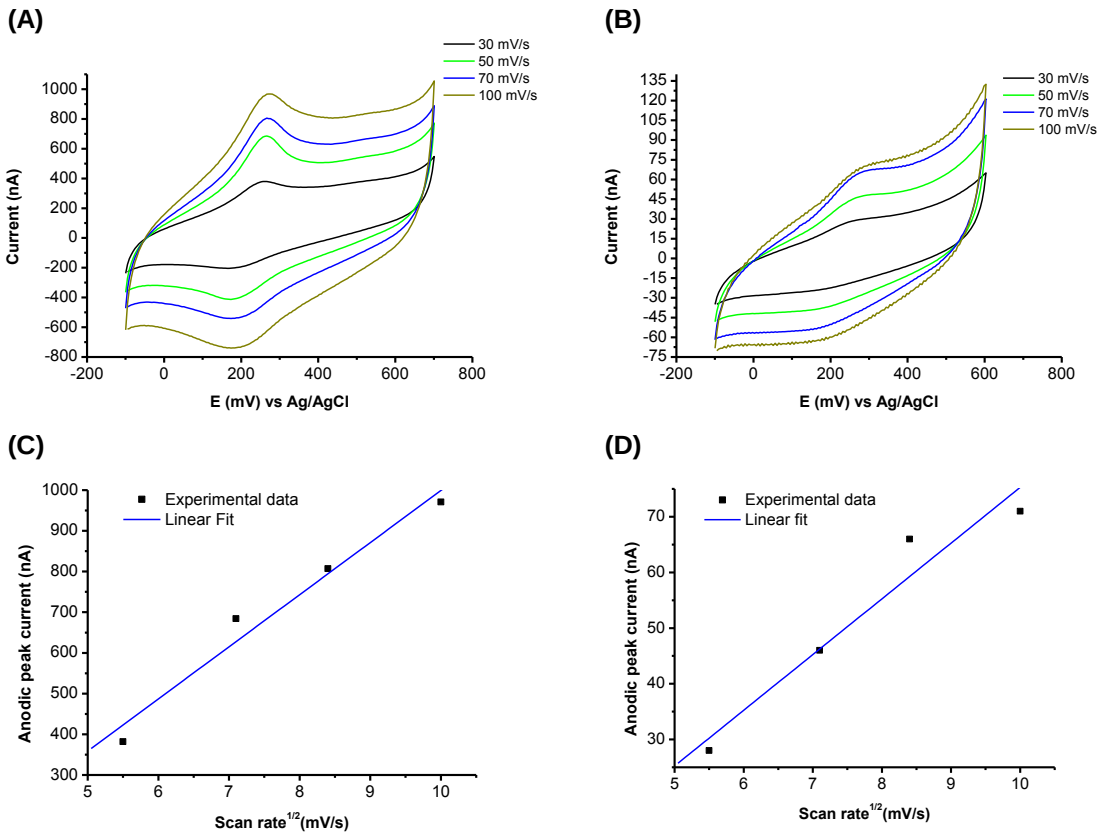

Figure 5.3 Cyclic voltammetry curves characterizing the redox activity of vinylferrocene in presence of GOx (A) and LOx (B) in the microneedles polymeric matrix at several scan rates; anodic peak current as function of square root of scan rate for vinylferrocene with GOx (C) and LOx (D).

As showed in Figure 5.3 (A) and Figure 5.3 (B), the two devices show anodic and cathodic peaks at about 300 and 200 mV, respectively, that are very close to typical peaks of free vinylferrocene (Ju et al., 1997). This result means that the polymeric matrix, containing GOx or LOx, does not interfere with the redox activity of the vinylferrocene. Figure 5.3 (A) and Figure 5.3 (B) also highlight that peak positions are unchanged as a function of scan rate and that reverse to forward peak current ratio is close to unity for both enzymatic electrodes.

Moreover, Figure 5.3 (C) and Figure 5.3 (D) demonstrate that the anodic peaks current increases proportionally to the scan rate (R^2 = 0.95 and R^2 = 0.91 respectively, R^2 being the coefficient of linear regression) for both enzymatic electrodes. These results suggest that the redox activity of the mediator is fast and reversible.

Chronoamperometry technique quantifies the responses, in terms of current, of the two devices at several concentrations of glucose and lactic acid, in concentration ranges of interest for the detection in human interstitial fluid (Shim et al., 2009; Shum et al., 2009; Yao et al., 2011; Thomas et al., 2012). During chronoamperometry measurements, the potential between working and reference electrodes is fixed and the current, flowing between working and auxiliary electrodes, is measured as function of time. The chronoamperometry characteristics are performed at 300 mV, in presence of known analyte concentrations, 5 minutes after addition of each aliquot of analyte in order to allow the diffusion inside the electrolytic solution. Glucose and lactic acid are detected at the following concentrations: 0, 2, 4, 6, 8, 10, 12 mM and 0, 0.2, 0.4, 0.6, 0.8, 1, 2, 3, 5, 7, 9, 12 mM, respectively. Figure 5.4 (A) and Figure 5.4 (B) report the current-time relationship of the two devices at several concentrations of glucose and lactic acid, respectively.

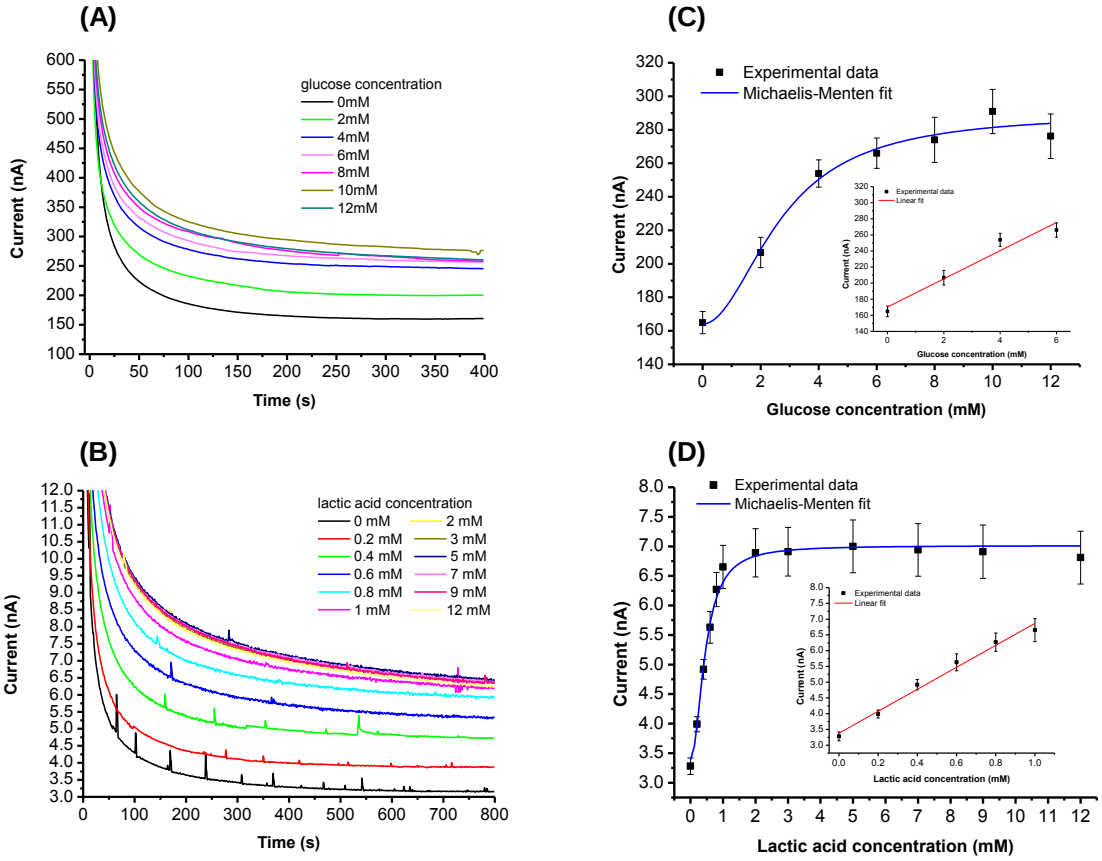

Figure 5.4 Chronoamperometry response of the microneedles based enzymatic electrodes at several concentrations of glucose (A) and lactic acid (B); calibrations curves and fits with Michaelis-Menten model of

the microneedles based enzymatic electrodes containing GOx (C) and LOx (D). In the inset of (C) and (D), the linear region of the response is underlined and the linear fit is showed.

Figure 5.4 (C) and Figure 5.4 (D) illustrate the calibration curves for glucose and lactic acid, respectively: for each analyte concentration, the stationary current value is considered. The response of the device to glucose is linear (R^2 value of 0.93) with a sensitivity of 18 ± 3 nA mM^{-1} in the range from 0 to 6 mM (see inset Figure 5.4 (C)). The response of the other device to lactic acid is linear (R^2 value of 0.98) with a sensitivity of 3.5 ± 0.2 nA mM^{-1} in the range from 0 to 1 mM (see inset Figure 5.4 (D)). Response times are of the order of minutes, and they depended on polymer nanostructure: penetration of solution in the microneedle matrix is diffusion-driven and faster signal generation can be obtained by tuning its porosity. By using a PEGDA with average molecular weight greater than 250, with longer polymeric chains and wider mesh, should promote analyte penetration and fasten device response. However, PEGDA molecular weight determines microneedles mechanical properties, such as indentation hardness; therefore, a tradeoff between analytes diffusion and penetration of the microneedles in human skin without breaking could limit the amount of PEGDA in the polymeric solution. The experimental data in Figure 5.4 (C) and Figure 5.4 (D) are fitted with Michaelis-Menten model for enzymatic kinetic behavior: $I=(I_{max} \cdot c) / (K_M + c)$, where I is the current response of the device, c is the analyte concentration and K_M is the Michaelis constant. The fits yield a K_M value of 2.7 ± 0.7 mM (R^2 = 0.99) in case of glucose, and 0.45 ± 0.03 mM (R^2 = 0.99) in case of lactic acid. The K_M represents a measure of how strong is the biomolecular interaction between the enzyme and the analyte: the obtained low values are related to the high affinity between the enzyme (GOx or LOx) and analyte (glucose or lactic acid), confirming that polymeric matrix allow the penetration of the analyte inside it and a correct working of the enzyme, even if confined in a nanometric space. The limits of detection, experimentally measured, is 1 µM for both the two analytes, quantifies by respective devices.

6. Filtration of small molecules by filter based microfluidic device

Since 1990, microfluidics has nowadays developed into a versatile technology with a huge plethora of applications. While initially focused on liquid and gases flow through simple channel layouts, designs of chips are much more complicated since they could include lot of components integrated inside. Large effort has been spent into the integration of unit operations on-chip, e.g. sample pre-treatment, mixing of different substances, controlled chemical reaction, and separation/purification of products (Sato et al., 2003; Erickson et al., 2004). Looking at methods used for components integration, many research groups have started out with clever designs of silicon chips, using the well-established toolbox of semiconductor industry. Lately, a shift toward new approaches increased, aimed to simple straightforward integration: mainly application of functionalized coatings, adsorption beads and filters. The use of filters in microfluidics is a topic of growing interest. Filter science and technology is a broad and highly interdisciplinary field, where process engineering, material science and chemistry meet all together. Exploring the boundaries of these fields offers many opportunities, and filters have already been used for an impressive range of functions, such as separation, purification, dialysis, and so on (Scrimgeour et al., 2011; Che et al., 2013). Traditional methods for improving components that can perform separation inside a microchannel include fabricating a barrier with reduced channel width (Brody et al., 1996) or an array of posts (He et al., 1999). While these approaches are capable of providing a reusable filter, the fabrication process can be time consuming and even expensive. Other way to fabricate a filter is to create a packed bed column, either by packing beads (Lettieri et al., 2003) or by *in situ* photopolymerization (Paustian et al., 2013). The *in situ* photopolymerization allows to control the position and thickness of the filter, simply by controlling the position and the parameters of the UV exposure. The pore size of produced filters depends of the ratio of the quantities of components contained in the hydrogel and of the exposure time to UV light. An additional advantage of this method is its application in existing device formats, provided that the used material for make the device is transparent to UV light. Disadvantages include the limited range of materials that can be applied. Filters can be fabricated using many soft materials such as PDMS, hydrogels and so on. As already mentioned, hydrogels based on PEGDA are particularly attractive due to the possibility of photo-induced cross-linking by simply adding a photoinitiator in the polymer solution.

In this chapter results on the microfluidic filter, fabricated as described in the paragraph 2.6, made inside the microfluidic device, fabricated as described in the paragraph 2.2, are presented. Also the plastic photomask used to make filter, as described in the paragraph 2.6, is presented. The operation of the filter is characterized allowing it to filter fluorescent molecules of rhodamine.

6.1. Plastic photomask

The fabrication process, described in the paragraph 2.6, allows to fabricate plastic photomasks with minimum feature achievable of about 20 μm, therefore it is particularly suitable for the fast prototyping of microfluidic devices. A test pattern, containing lines and dots in black and white with dimensions from 10 to 100 μm, is designed (see Figure 6.1 (A)) and transferred onto photographic film (see Figure 6.1 (B)) using this process.

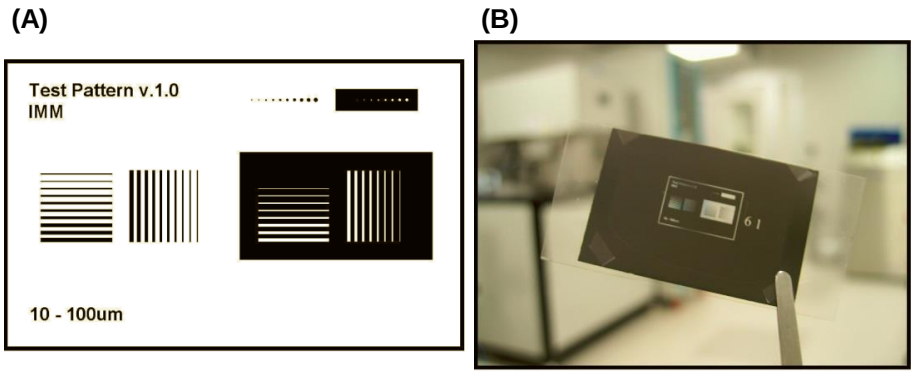

Figure 6.1 (A) Test pattern; (B) plastic photomask.

Figure 6.2 (A) shows in details the plastic photomask, in which the edge are not so straight and well defined and there is a transition region of few microns from dark to transparent region. Dark regions are due to the presence of small particles of a metallic silver, or dye clouds (see Figure 6.2 (B)), developed from silver halide that have received enough white light. It is possible to observe the film grain, that has an average thickness of 410 nm and a roughness of 120 nm (see Figure 6.2 (C)). However in transparent regions where silver is absent, black dots with a diameter from 0.4 to 3.2 μm are found. These defects can be neglected for microfluidic applications.

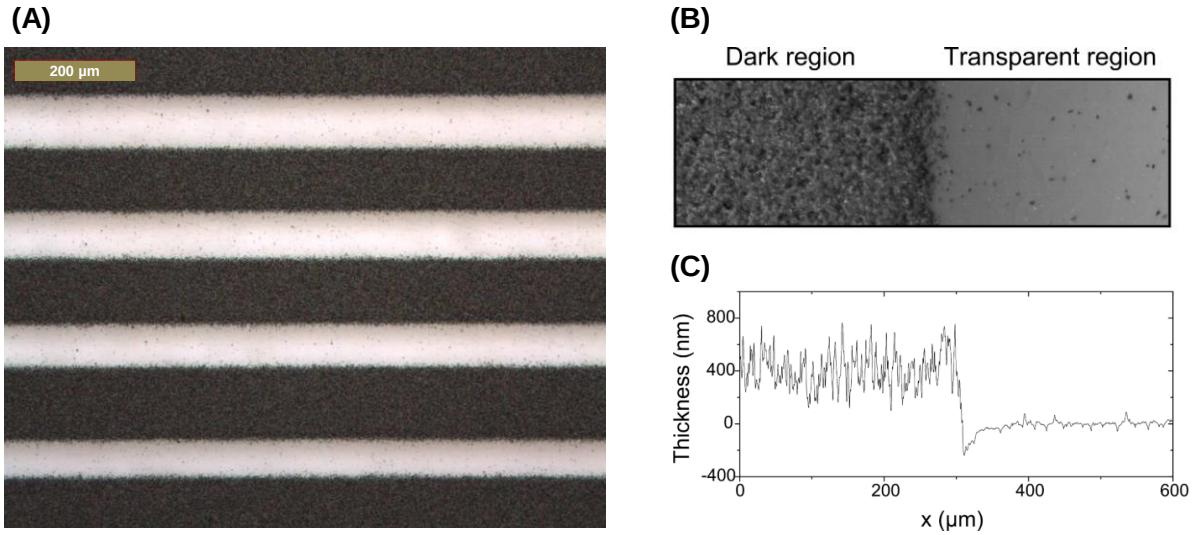

Figure 6.2 (A) Optical image of the plastic photomask; zoom (B) and thickness profile (C) of the transition from dark to transparent regions.

6.2. Filter based microfluidic device

Most of the microfluidic devices are made of PDMS, since it combines numerous excellent physical and chemical properties (Bartolo et al., 2008). Nevertheless, some of the properties of PDMS strongly limit its range of applications. For example, this silicone elastomer swells in most organic solvents that is the major constraint to its use in aqueous solutions. Moreover, permanent modification of PDMS surfaces chemical properties is still a challenging task. Finally, the low elastic modulus of PDMS does not allow the use of high pressure (> 1 bar) operations. In order to overcome these problems, microfluidic devices can be fabricated using NOA. Figure 6.3 shows the microfluidic device in NOA fabricated by soft imprint lithography, described in the paragraph 2.2.

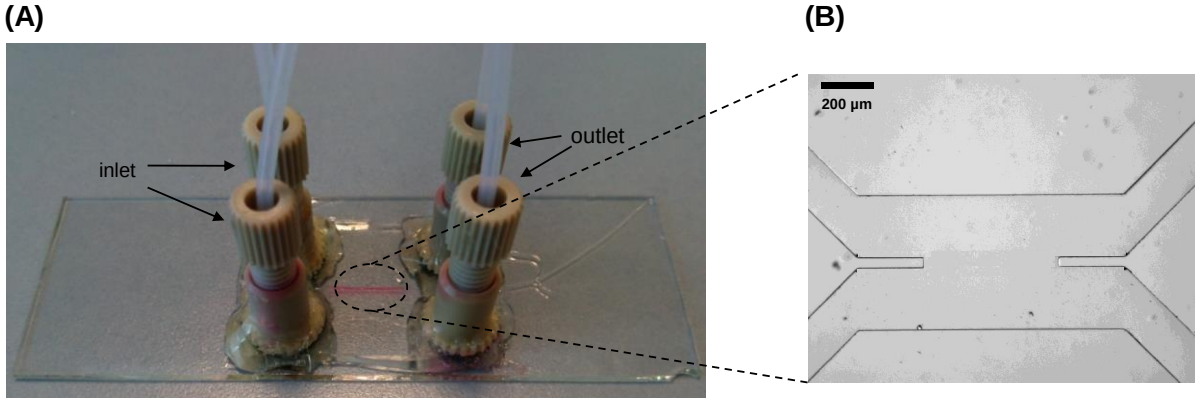

Figure 6.3 (A) Sketch of the microfluidic device; (B) zoom of the circuit.

Nanoports, that are plastic connectors which allow to seal plastic tubes for the injection of the liquids, are glued on the inlets and outlets of the circuit.

The microfluidic device is integrated with a filter, fabricated as described in the paragraph 2.6. The final microfluidic circuit, showed in Figure 6.4, is thus constituted by two channels (height=25 µm, width=225 µm) separated by the filter with height of 25 µm and width of 50 µm.

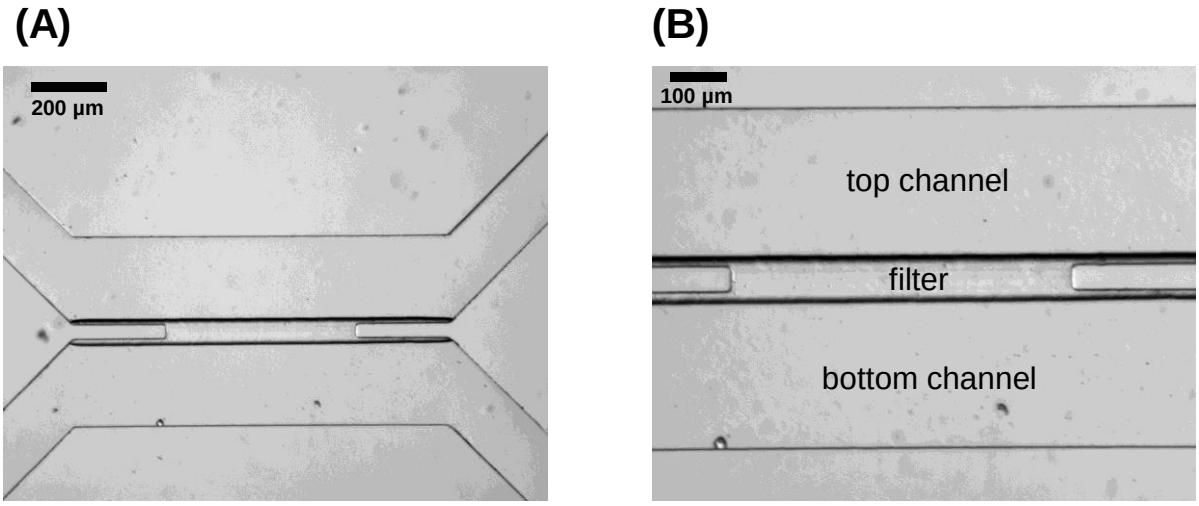

Figure 6.4 (A) Image of the microfluidic circuit, constituted by the two channels and the filter; (B) zoom of the circuit, where the filter separates the top channel from the bottom channel.

6.3. Optically monitored filtration of rhodamine molecules

In order to see the operation of the filter, fluorescence molecules of rhodamine 6G (R6G) are filtered. The functioning of the filter is characterized in the following (see Figure 6.5).

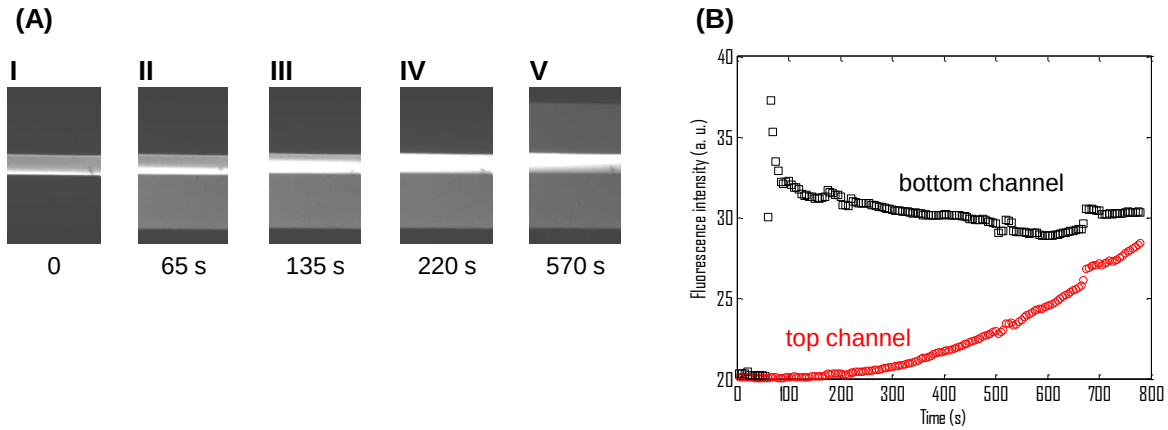

Figure 6.5 Operation of the filter at Q=500 µL/min: fluorescence images (A) and intensities (B) of the two channels as function of time.

The two channels are filled with water at flow rate Q of 500 µL/min for some minutes in order to clean them. Then, the flow of water in the top channel is stopped ($Q \sim 0$) and the same channel is left filled of water. Since water is not fluorescent, the two channels are not

fluorescent (see Figure 6.5 (A) I). The bottom channel is filled with an aqueous solution of R6G at *Q*=500 µL/min, therefore it becomes completely fluorescent (see Figure 6.5 (A) II). The R6G diffuses from the bottom to the top channel through the filter (see Figure 6.5 (A) III, IV). After few minutes, the top channel is filled of the R6G (see Figure 6.5 (A) V) therefore it becomes completely fluorescent. Figure 6.5 (B) shows the fluorescence intensities as function of the time of the bottom and top channels: the intensities tend to become equals after a few minutes.

The reversibility of the device is showed in Figure 6.6.

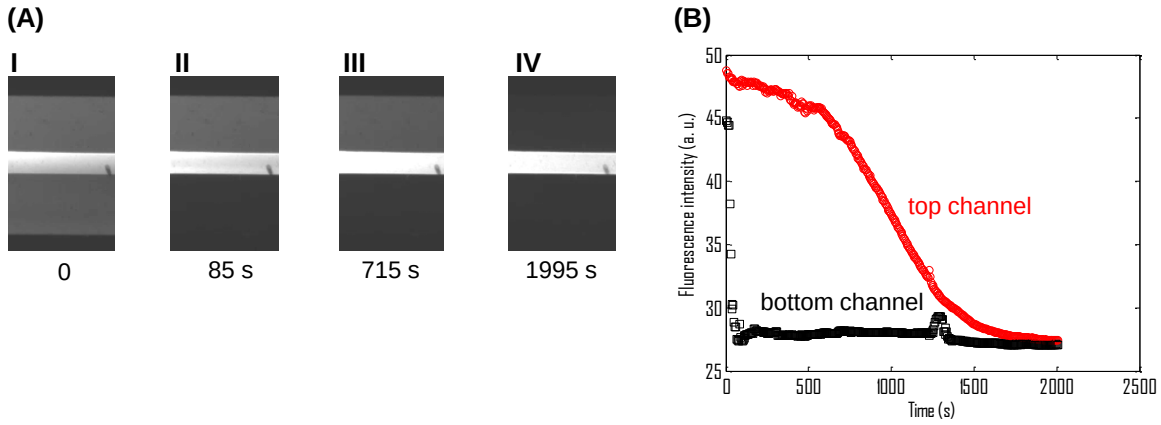

Figure 6.6 Reversibility of the filter at *Q*=500 µL/min: fluorescence images (A) and intensities (B) of the two channels as function of time.

The two channels, containing an aqueous solution of R6G (*Q* ~ 0 in the top channel) from the previous test, are fluorescent (see Figure 6.6 (A) I). The bottom channel is filled with water at *Q*=500 µL/min, therefore it becomes completely not fluorescent (see Figure 6.6 (A) II). The water diffuses from the bottom to the top channel through the filter (see Figure 6.6 (A) III). After few minutes, the top channel is filled of water therefore it becomes completely not fluorescent. Figure 6.6 (B) shows the fluorescence intensities as function of the time of the bottom and top channels: the intensities tend to become equals after a few minutes.

The same studies were performed by tuning the solution flux at *Q*=100 µL/min (see Figure 6.7 and Figure 6.8).

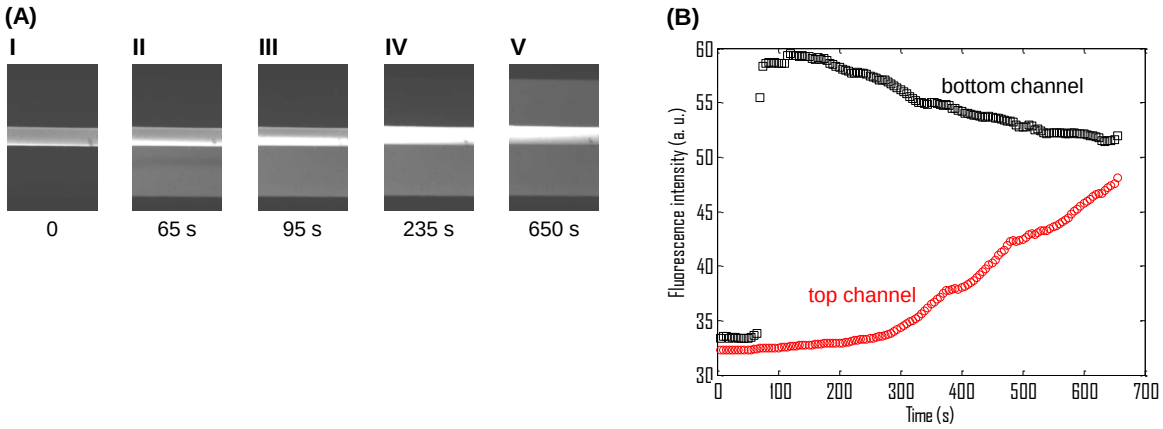

Figure 6.7 Operation of the filter at *Q*=100 µL/min: fluorescence images (A) and intensities (B) of the two channels as function of time.

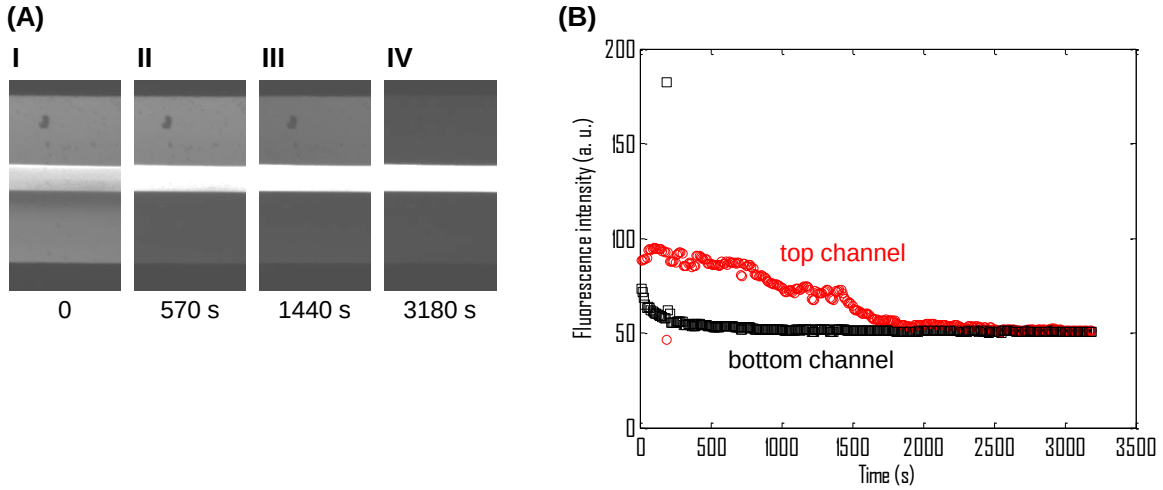

Figure 6.8 Reversibility of the filter at *Q*=100 µL/min: fluorescence images (A) and intensities (B) of the two channels as function of time.

The behavior of the system is very similar to the previous one and significant differences cannot been seen.

7. Conclusions

Well established integrated circuits technologies, traditionally used in production of microprocessors, are more and more exploited in different fields, very distant from classic electronics, such as medicine and biology. However, transferring these technologies from the integrated circuit industry to other scientific fields is not trivial, since it requires large efforts to adapt traditional materials and processes to these areas or in some cases to develop and use alternative materials and processes with respect to traditional ones. Nevertheless, the research towards this direction offers amazing potentialities. For example, it gives a unique opportunity to fabricate miniaturized devices for a huge variety of applications, like the realization of microdevices that have the same functionalities of a conventional laboratory equipment, or, in the better cases, the integration of all laboratory functions in a single microdevice, the development of tools to make tasks in more efficient and effective way with respect to conventional methods, and in some cases in real time and in continuous mode. The research activity presented in this PhD thesis is placed in this contest with the aim to define new fabrication procedures, combining lithographic processes of both hard and soft materials, for the realization of three innovative microdevices for biomedical applications.

The firsts two microdevices, one for transdermal drug delivery and the other for transdermal biosensing, have been fabricated by photolithography. The core of these microdevices is the flexible microneedle array. Microneedles have been fabricated with only the photolithographic process of a photocurable hydrogel based on PEGDA. No other step, like thin layers deposition or etching has been used, thus making the process simple, fast and cheap. Microneedles with several heights, bases and curvature radii of the tips have been fabricated by changing the UV light intensity or the exposure time to UV light. The height varies from about 200 to 2200 μm, the bases are 250 μm and 400 μm, and the curvature radius goes from about 2 to 11 μm. Indentation hardness of the microneedles has been compared with that of a parafilm M, used as artificial skin very similar to the surface layer of the pig skin. Microneedles have an indentation hardness more high than that of the parafilm M, thus they are able to penetrate into the skin. A penetration test of microneedles into eight parafilm M layers folded on self, that mimics the pig skin, has been performed. Microneedles penetrate the first four layers, for a total distance of 640 μm, without breaking.

The first microdevice, made of a free-standing porous silicon membrane integrated with a microneedle array, has been realized and tested for the releasing of fluorescein molecules, which can mimic a small drug, into a PBS solution, that mimics the human interstitial fluid.

7. Conclusions

The fluorescein molecules have been loaded in the porous silicon membrane, which acts as a drug reservoir. At the same time, it allows an optical control of the drug loading since the reflectivity spectra of the porous silicon membrane red shifts of about 100 nm. Fluorescein molecules diffuse from the porous silicon reservoir to the microneedles: this has been confirmed by spectroscopic reflectometry, evidencing a blue shift of about 50 nm of the reflectivity spectra of the porous silicon membrane, and by strong fluorescence exhibited by microneedle array. The shifts of the reflectivity spectra correspond to changes in color of the porous silicon membrane, visible by naked eye, from violet to green and then to blue. The diffusion of the fluorescein molecules from the microneedles into the PBS solution has been confirmed by the continuous decreasing of the fluorescence intensity of the microneedles during the immersion of the device in PBS solution for 2, 4, 8 and 24 hours. Migration of fluorescein molecules from porous silicon reservoir to microneedles, and from microneedles to PBS solution is only driven by diffusion and conditioned by material properties and morphologies: by tuning porosities of silicon and polymer, and changing their surface chemistries, every kind of drug (hydrophilic and lipophilic) in any interval of time (very rapid or very slow) can be locally administrated without using any external force.

The second set of microdevices, i.e. microneedles based enzymatic electrodes, made of microneedle arrays coated by gold, has been realized and tested for electrochemical detection of glucose and lactic acid molecules. The microneedle array of both electrodes contains a redox mediator, the vinylferrocene. Moreover, the microneedle array of the electrode for the detection of glucose also contains the enzyme GOx, while the other microdevice contains the LOx. The redox activity of the vinylferrocene, that carries electrons from the enzyme to the surface electrode, has been checked by cyclic voltammetry. These measurements show that anodic and cathodic peaks of vinylferrocene, immobilized inside the microneedles, are 300 mV and 200 mV, for both microdevices. These values are the typical peak values of the free vinylferrocene, therefore the polymeric matrix and the other species contained inside the microneedles do not affect the redox activity of vinylferrocene. The two microdevices have been used to quantify glucose and lactic acid in PBS solutions with concentrations of analytes in the mM range, which is the range of interest in the human interstitial fluid in physiologic conditions. The calibration curves, i.e. current as function of analyte concentration, show good sensitivities, 18 ± 3 nA mM^{-1} and 3.5 ± 0.2 nA mM^{-1} for the detection of glucose and lactic acid, respectively. Since the two microdevices have an enzymatic behavior, the experimental data of the calibration curves have been fitted by Michaelis-Mentel model: the fits yielded a K_M value of 2.7 ± 0.7 mM in case of glucose and 0.45 ± 0.03 mM in case of

lactic acid. The K_M estimated are low, which means that there is a high affinity between the enzyme (GOx or LOx) immobilized inside the microneedles and the analyte (glucose or lactic acid), therefore the activity of the immobilized enzyme is not altered compared to the free enzyme. The limit of detection, experimentally measured, is 1 µM for both the two analytes, quantified by respective microdevices.

A homemade fabrication process, based on photographic reduction technique, of photomasks on photographic films for fast prototyping of microfluidic devices has been developed. This process allows the fabrication of cheap plastic photomasks, with a spatial resolution of about 20 µm.

The third microdevice, made of a microfluidic device with a microfluidic filter inside, has been realized and tested for the filtration of fluorescent small molecules of R6G. The microfluidic device has been realized in NOA by soft imprint lithography, that overcomes the PDMS limits and extends the range of its applications, which is the basic material in the microfluidic field. The device is constituted by two channels, with height of 25 µm and width of 225 µm. The microfluidic filter has been realized inside the microfluidic device by *in situ* photopolymerization of a photocurable hydrogel based on PEGDA using a homemade plastic photomask. The advantages of this process are simplicity, speed, and versatility due to the possibility of fabricating the filter in any location of any microfluidic circuit. Moreover, it allows the use of several standard UV exposure systems, like a microscope coupled with a UV lamp, a mask aligner traditionally used for photolithography or a microscope coupled to a DMD and a UV lamp. The filter has a height of 25 µm and a width of 50 µm. The operation of the filter has been tested: the fluorescent molecules of R6G diffuse from one channel to the other channel through the filter, that is constituted of nanopores. Two different flow rates have been used, in particular 100 µL/min e 500 µL/min: significant differences between them have been not seen. Other characterizations have to be done in order to provide quantitative parameters of the filter, like permeability, by measuring the flow rate and the diffusion time, in order to allow the use of this microdevice for a specific biomedical application, like microdialysis.

Even if not straightforward nor simple, the shifting of existing and mature technologies from the consumer electronics to biomedical world can led to the creation of novel microdevices and tools with excellent characteristics and functionalities. However, standard production of microdevices and tools that can really replace the existing equipment and methods is still far. For evidence of this, it can think to the computer mouse, which took 20 years to appear in the Macintosh computer after its first prototype made in the 1960s by Engelbart. Therefore, the

research, both basic and applied, in this field is active and promising, and others exceptional results can be envisaged.

8. References

Aoyagi, S., Izumi, H., & Fukuda, M. (**2008**). Biodegradable polymer needle with various tip angles and consideration on insertion mechanism of mosquito's proboscis. *Sensors and Actuators A: Physical*, *143*(1), 20-28.

Ashraf, M. W., Tayyaba, S., & Afzulpurkar, N. (**2011**). Micro electromechanical systems (MEMS) based microfluidic devices for biomedical applications. *International journal of molecular sciences*, *12*(6), 3648-3704.

Ashraf, M. W., Tayyaba, S., Nisar, A., Afzulpurkar, N., Bodhale, D. W., Lomas, T., Poyai, A., & Tuantranont, A. (**2010**). Design, fabrication and analysis of silicon hollow microneedles for transdermal drug delivery system for treatment of hemodynamic dysfunctions. *Cardiovascular Engineering*, *10*(3), 91-108.

Aspnes, D. E., Theeten, J. B., & Hottier, F. (**1979**). Investigation of effective-medium models of microscopic surface roughness by spectroscopic ellipsometry. *Physical Review B*, *20*(8), 3292.

Bartolo, D., Degré, G., Nghe, P., & Studer, V. (**2008**). Microfluidic stickers. *Lab on a Chip*, *8*(2), 274-279.

Betancourt, T., & Brannon-Peppas, L. (**2006**). Micro-and nanofabrication methods in nanotechnological medical and pharmaceutical devices. *International journal of nanomedicine*, *1*(4), 483.

Bhandari, R., Negi, S., & Solzbache, F. (**2008**, May). A novel mask-less method of fabricating high aspect ratio microneedles for blood sampling. In *Electronic Components and Technology Conference, 2008. ECTC 2008. 58th*(pp. 1306-1309). IEEE.

Bhansali, S., & Vasudev, A. (Eds.). (**2012**). *MEMS for biomedical applications*. Elsevier.

Brody, J. P., Osborn, T. D., Forster, F. K., & Yager, P. (**1996**). A planar microfabricated fluid filter. *Sensors and Actuators A: Physical*, *54*(1), 704-708.

Campbell, P. K., Jones, K. E., Huber, R. J., Horch, K. W., & Normann, R. (**1991**). A silicon-based, three-dimensional neural interface: manufacturing processes for an intracortical electrode array. *Biomedical Engineering, IEEE Transactions on*, *38*(8), 758-768.

Cevc, G. (**2004**). Lipid vesicles and other colloids as drug carriers on the skin. *Advanced drug delivery reviews*, *56*(5), 675-711.

Chandrasekaran, S. (**2003**). Characterization of surface micromachined metallic microneedles. *Microelectromechanical Systems, Journal of*, *12*(3), 289-295.

Che, J., Mach, A. J., Go, D. E., Talati, I., Ying, Y., Rao, J., Kulkarni, R. P., & Di Carlo, D. (**2013**). Microfluidic purification and concentration of malignant pleural effusions for improved molecular and cytomorphological diagnostics.

Chen, B., Wei, J., & Iliescu, C. (**2010**). Sonophoretic enhanced microneedles array (SEMA)-Improving the efficiency of transdermal drug delivery. *Sensors and Actuators B: Chemical*, *145*(1), 54-60.

Davis, G. (**2008**). Microfluidics: its impact on drug discovery. *Innov. Pharm. Technol.*, *25*, 24-27.

Davis, S. P., Landis, B. J., Adams, Z. H., Allen, M. G., & Prausnitz, M. R. (**2004**). Insertion of microneedles into skin: measurement and prediction of insertion force and needle fracture force. *Journal of biomechanics*, *37*(8), 1155-1163.

De Jong, J., Lammertink, R. G. H., & Wessling, M. (**2006**). Membranes and microfluidics: a review. *Lab on a Chip*, *6*(9), 1125-1139.

Denet, A. R., Vanbever, R., & Préat, V. (**2004**). Skin electroporation for transdermal and topical delivery. *Advanced drug delivery reviews*, *56*(5), 659-674.

Dhanekar, S., & Jain, S. (**2013**). Porous silicon biosensor: Current status. *Biosensors and Bioelectronics*, *41*, 54-64.

Donnelly, R. F., Singh, T. R. R., Garland, M. J., Migalska, K., Majithiya, R., McCrudden, C. M., Kole, P. L., Mahmood, T. M. T., McCarthy, H. O., & Woolfson, A. D. (**2012**). Hydrogel-forming microneedle arrays for enhanced transdermal drug delivery. *Advanced functional materials*, *22*(23), 4879-4890.

Donnelly, R. F., Singh, T. R. R., Tunney, M. M., Morrow, D. I., McCarron, P. A., O'Mahony, C., & Woolfson, A. D. (**2009**). Microneedle arrays allow lower microbial penetration than hypodermic needles in vitro. *Pharmaceutical research*, *26*(11), 2513-2522.

Doukas, A. G., & Kollias, N. (**2004**). Transdermal drug delivery with a pressure wave. *Advanced drug delivery Reviews*, *56*(5), 559-579.

Erickson, D., & Li, D. (**2004**). Integrated microfluidic devices. *Analytica Chimica Acta*, *507*(1), 11-26.

Gates, B. D., Xu, Q., Stewart, M., Ryan, D., Willson, C. G., & Whitesides, G. M. (**2005**). New approaches to nanofabrication: molding, printing, and other techniques. *Chemical reviews*, *105*(4), 1171-1196.

He, B., Tan, L., & Regnier, F. (**1999**). Microfabricated filters for microfluidic analytical systems. *Analytical Chemistry*, *71*(7), 1464-1468.

Heller, A., & Feldman, B. (**2008**). Electrochemical glucose sensors and their applications in diabetes management. *Chemical reviews*, *108*(7), 2482-2505.

Ju, H., & Leech, D. (**1997**). Electrochemistry of poly (vinylferrocene) formed by direct electrochemical reduction at a glassy carbon electrode. *Journal of the Chemical Society, Faraday Transactions*, *93*(7), 1371-1375.

Kalia, Y. N., Naik, A., Garrison, J., & Guy, R. H. (**2004**). Iontophoretic drug delivery. *Advanced drug delivery reviews*, *56*(5), 619-658.

Kochhar, J. S., Goh, W. J., Chan, S. Y., & Kang, L. (**2013**). A simple method of microneedle array fabrication for transdermal drug delivery. *Drug development and industrial pharmacy*, *39*(2), 299-309.

Langer, R. (**2001**). Drugs on target. *Science*, *293*(5527), 58-59.

Larrañeta, E., Moore, J., Vicente-Pérez, E. M., González-Vázquez, P., Lutton, R., Woolfson, A. D., & Donnelly, R. F. (**2014**). A proposed model membrane and test method for microneedle insertion studies. *International journal of pharmaceutics*, *472*(1), 65-73.

Lee, J. W., Park, J. H., & Prausnitz, M. R. (**2008**). Dissolving microneedles for transdermal drug delivery. *Biomaterials*, *29*(13), 2113-2124.

Lettieri, G. L., Dodge, A., Boer, G., de Rooij, N. F., & Verpoorte, E. (**2003**). A novel microfluidic concept for bioanalysis using freely moving beads trapped in recirculating flows. *Lab on a Chip*, *3*(1), 34-39.

Li, H., Yu, Y., Faraji Dana, S., Li, B., Lee, C. Y., & Kang, L. (**2013**). Novel engineered systems for oral, mucosal and transdermal drug delivery. *Journal of drug targeting*, *21*(7), 611-629.

Lipomi, D. J., Martinez, R. V., Cademartiri, L., & Whitesides, G. M. (**2012**). 7.11-Soft Lithographic Approaches to Nanofabrication. *Polymer Science: A Comprehensive Reference, Ed. K. Matyjaszewski and M. Möller, Elsevier, Amsterdam*.

Liu, Y., Eng, P. F., Guy, O. J., Roberts, K., Ashraf, H., & Knight, N. (**2013**). Advanced deep reactive-ion etching technology for hollow microneedles for transdermal blood sampling and drug delivery. *IET nanobiotechnology*, *7*(2), 59-62.

Matteucci, M., Casella, M., Bedoni, M., Donetti, E., Fanetti, M., De Angelis, F., Gramatica, F., & Di Fabrizio, E. (**2008**). A compact and disposable transdermal drug delivery system. *Microelectronic Engineering*, *85*(5), 1066-1073.

McDonald, J. C., & Whitesides, G. M. (**2002**). Poly (dimethylsiloxane) as a material for fabricating microfluidic devices. *Accounts of chemical research*, *35*(7), 491-499.

Mehta, G., Lee, J., Cha, W., Tung, Y. C., Linderman, J. J., & Takayama, S. (**2009**). Hard top soft bottom microfluidic devices for cell culture and chemical analysis. *Analytical chemistry*, *81*(10), 3714-3722.

MicroChem. www.microchem.com

Milewski, M., Brogden, N. K., & Stinchcomb, A. L. (**2010**). Current aspects of formulation efforts and pore lifetime related to microneedle treatment of skin. *Expert opinion on drug delivery*, *7*(5), 617-629.

Mitragotri, S., & Kost, J. (**2004**). Low-frequency sonophoresis: a review. *Advanced drug delivery reviews*, *56*(5), 589-601.

Mukerjee, E. V., Collins, S. D., Isseroff, R. R., & Smith, R. L. (**2004**). Microneedle array for transdermal biological fluid extraction and in situ analysis. *Sensors and Actuators A: Physical*, *114*(2), 267-275.

Norland Products. www.norlandprod.com

Nunes, G. S., & Marty, J. L. (**2006**). Immobilization of enzymes on electrodes. In *Immobilization of Enzymes and Cells* (pp. 239-250). Humana Press.

Oh, J. H., Park, H. H., Do, K. Y., Han, M., Hyun, D. H., Kim, C. G., Kim, C. H., Lee, S. S., Hwang, S. J., Shin, S. C., & Cho, C. W. (**2008**). Influence of the delivery systems using a microneedle array on the permeation of a hydrophilic molecule, calcein. *European Journal of Pharmaceutics and Biopharmaceutics*, *69*(3), 1040-1045.

Oh, J. K. (**2009**). Engineering of nanometer-sized cross-linked hydrogels for biomedical applications. *Canadian Journal of Chemistry*, *88*(3), 173-184.

Ottosen, R. M. (**1999**). Replication and compression of surface structures with polydimethylsiloxane elastomer. *Journal of Chemical Education*, *76*(4), 537.

Paustian, J. S., Azevedo, R. N., Lundin, S. T. B., Gilkey, M. J., & Squires, T. M. (**2013**). Microfluidic microdialysis: spatiotemporal control over solution microenvironments using integrated hydrogel membrane microwindows. *Physical Review X*, *3*(4), 041010.

Pishko, M. V., Michael, A. C., & Heller, A. (**1991**). Amperometric glucose microelectrodes prepared through immobilization of glucose oxidase in redox hydrogels. *Analytical Chemistry*, *63*(20), 2268-2272.

Qin, D., Xia, Y., & Whitesides, G. M. (**2010**). Soft lithography for micro-and nanoscale patterning. *Nature protocols*, *5*(3), 491-502.

Quake, S. R., & Scherer, A. (**2000**). From micro-to nanofabrication with soft materials. *Science*, *290*(5496), 1536-1540.

Rajaraman, S., & Henderson, H. T. (**2005**). A unique fabrication approach for microneedles using coherent porous silicon technology. *Sensors and Actuators B: Chemical*, *105*(2), 443-448.

Rogers, J. A., & Nuzzo, R. G. (**2005**). Recent progress in soft lithography. *Materials today*, *8*(2), 50-56.

Sachdeva, V., & K Banga, A. (**2011**). Microneedles and their applications. *Recent patents on drug delivery & formulation*, *5*(2), 95-132.

Sailor, M. J. (**2012**). *Porous silicon in practice: preparation, characterization and applications*. John Wiley & Sons.

Sato, K., Hibara, A., Tokeshi, M., Hisamoto, H., & Kitamori, T. (**2003**). Microchip-based chemical and biochemical analysis systems. *Advanced Drug Delivery Reviews*, *55*(3), 379-391.

Scrimgeour, J., Cho, J. K., Breedveld, V., & Curtis, J. (**2011**). Microfluidic dialysis cell for characterization of macromolecule interactions. *Soft Matter*, *7*(10), 4762-4767.

Shibata, T., Nakanishi, A., Sakai, T., Kato, N., Kawashima, T., Mineta, T., & Makino, E. (**2007**, June). Fabrication and mechanical characterization of microneedle array for cell surgery. In *Solid-State Sensors, Actuators and Microsystems Conference, 2007. TRANSDUCERS 2007. International* (pp. 719-722). IEEE.

Shim, N. Y., Bernards, D. A., Macaya, D. J., DeFranco, J. A., Nikolou, M., Owens, R. M., & Malliaras, G. G. (**2009**). All-plastic electrochemical transistor for glucose sensing using a ferrocene mediator. *Sensors*, *9*(12), 9896-9902.

Shum, A. J., Cowan, M., Lähdesmäki, I., Lingley, A., Otis, B., & Parviz, B. A. (**2009**, August). Functional modular contact lens. In *SPIE NanoScience+ Engineering* (pp. 73970K-73970K). International Society for Optics and Photonics.

Smith, R. L., & Collins, S. D. (**1992**). Porous silicon formation mechanisms. *Journal of Applied Physics*, *71*(8), R1-R22.

Sze, S. M. (**2008**). *Semiconductor devices: physics and technology*. John Wiley & Sons.

Thomas, N., Lähdesmäki, I., & Parviz, B. A. (**2012**). A contact lens with an integrated lactate sensor. *Sensors and Actuators B: Chemical*, *162*(1), 128-134.

Touitou, E. (**2002**). Drug delivery across the skin. *Expert opinion on biological therapy*, *2*(7), 723-733.

Tsuchiya, K., Nakanishi, N., Uetsuji, Y., & Nakamachi, E. (**2005**). Development of blood extraction system for health monitoring system. *Biomedical microdevices*, *7*(4), 347-353.

Valdés-Ramírez, G., Windmiller, J. R., Claussen, J. C., Martinez, A. G., Kuralay, F., Zhou, M., Zhou, N., Polsky, R., Miller, P. R., Narayan, R., & Wang, J. (**2012**). Multiplexed and switchable release of distinct fluids from microneedle platforms via conducting polymer nanoactuators for potential drug delivery. *Sensors and Actuators B: Chemical*, *161*(1), 1018-1024.

Ventrelli, L., Marsilio Strambini, L., & Barillaro, G. (**2015**). Microneedles for transdermal biosensing: current picture and future direction. *Advanced healthcare materials*, *4*(17), 2606-2640.

Wang, J. (**2008**). Electrochemical glucose biosensors. *Chemical reviews*, 2008, *108*(2), 814-825.

Wilke, N., Hibert, C., O'Brien, J., & Morrissey, A. (**2005**). Silicon microneedle electrode array with temperature monitoring for electroporation. *Sensors and Actuators A: Physical*, *123*, 319-325.

Williams, A. C., & Barry, B. W. (**2012**). Penetration enhancers. *Advanced drug delivery reviews*, *64*, 128-137.

Yan, J., Pedrosa, V. A., Simonian, A. L., & Revzin, A. (**2010**). Immobilizing enzymes onto electrode arrays by hydrogel photolithography to fabricate multi-analyte electrochemical biosensors. *ACS applied materials & interfaces*, *2*(3), 748-755.

Yao, H., Shum, A. J., Cowan, M., Lähdesmäki, I., & Parviz, B. A. (**2011**). A contact lens with embedded sensor for monitoring tear glucose level. *Biosensors and Bioelectronics*, *26*(7), 3290-3296.

Ziaie, B., Baldi, A., Lei, M., Gu, Y., & Siegel, R. A. (**2004**). Hard and soft micromachining for BioMEMS: review of techniques and examples of applications in microfluidics and drug delivery. *Advanced drug delivery reviews*, *56*(2), 145-172.

Appendix A - Lists of publications and research experiences in external labs related to the PhD work

List of publications

Journals

J5. Caliò, A., Dardano, P., Di Palma, V., Bevilacqua, M. F., Di Matteo, A., Iuele, H., & De Stefano, L. (2016). Polymeric microneedles based enzymatic electrodes for electrochemical biosensing of glucose and lactic acid. *Sensors and Actuators B: Chemical*, submitted paper.

J4. Dardano, P., **Caliò, A.**, Politi, J., Rea, I., Rendina, I., & De Stefano, L. (2016). Optically monitored drug delivery patch based on porous silicon and polymer microneedles. *Biomedical Optics Express*, accepted paper.

J3. Caliò, A., Leng, J., Decock, J., De Stefano, L., & Salmon, J. B. (2015). Microscopy assisted fabrication of a hydrogel-based microfluidic filter. *Journal of the European Optical Society-Rapid publications*, *10*. doi: 10.2971/jeos.2015.15058

J2. Dardano, P., **Caliò, A.**, Di Palma, V., Bevilacqua, M. F., Di Matteo, A., & De Stefano, L. (2015). A photolithographic approach to polymeric microneedles array fabrication. *Materials*, *8*(12), 8661-8673. doi: 10.3390/ma8125484

J1. Orabona, E., **Caliò, A.**, Rendina, I., Stefano, L. D., & Medugno, M. (2013). Photomasks fabrication based on optical reduction for microfluidic applications. *Micromachines*, *4*(2), 206-214. doi: 10.3390/mi4020206

Proceedings

P3. Dardano, P., Rea, I., De Stefano, L., **Caliò, A.**, & Politi, J., Optically controlled drug delivery system based on porous silicon and microneedles patch. In *NANOfIM 2015, 1st Workshop on Nanotechnology in Instrumentation and Measurement*, Lecce, 24-25 July 2015. ISBN 978-1-5108-1501-8

P2. Dardano, P., **Caliò, A.**, Politi, J., Di Palma, V., Bevilacqua, M. F., Rea, I., Casalino, M., Di Matteo, A., Rendina, I., & De Stefano, L. (2015, June). Hybrid microneedles devices for diagnostic and therapeutic applications: fabrication and preliminary results. In *SPIE Microtechnologies* (pp. 95180L-95180L). International Society for Optics and Photonics. doi:10.1117/12.2178919

P1. Dardano, P., **Caliò, A.**, Politi, J., Rea, I., De Stefano, L., Di Palma, V., Bevilacqua, M. F.,

& Di Matteo, A. (2015, February). Diagnostic and therapeutic devices based on polymeric microneedles: fabrication and preliminary results. In *AISEM Annual Conference, 2015 XVIII* (pp. 1-4). IEEE. doi:10.1109/AISEM.2015.7066782

List of research experiences in external labs

E2. Visiting student: Laboratory of the future - Solvay, Pessac (France)

Period: 03/01/2015 - 06/30/2015

Scientific supervisors: Jacques Leng, Jean-Baptiste Salmon

Research field: microfluidics

E1. Visiting student: STMicroelectronics, Arzano (Italy)

Period: once a week from 03/01/2013 to 02/29/2016

Scientific supervisors: Andrea Di Matteo, Vincenza Di Palma

Research field: microelectronics

Appendix B - List of publications related to the other research activities investigated during the PhD program

List of publications

Book chapter

B1. De Stefano, L., Rea, I., **Caliò, A.**, Politi, J., Terracciano, M., & Korotcenkov, G. (2015). Porous silicon-based optical chemical sensors. *Porous silicon: from formation to application: biomedical and sensor applications, volume two: Biomedical and sensor applications*, 69. doi: 10.1201/b19205

Journals

J5. Politi, J., Dardano, P., **Caliò, A.**, Iodice, M., Rea, I., & De Stefano, L. (2016). Lysine modified oligopeptides allow reversible sensing of lead (II) ions on chip. *Biosensors and Bioelectronics*, submitted paper.

J4. Della Ventura, B., Rea, I., **Caliò, A.**, Giardina, P., Gravagnuolo, A. M., Funari, R., Altucci, C., Velotta, R., & De Stefano, L. (2016). Vmh2 hydrophobin layer entraps glucose: a quantitative characterization by label-free optical and gravimetric methods. *Applied Surface Science*, *364*, 201-207. doi:10.1016/j.apsusc.2015.12.080

J3. Casalino, M., Coppola, G., De Stefano, L., **Caliò, A.**, Rea, I., Mocella, V., Dardano, P., Romano, S., Rao, S., & Rendina, I. (2015). New perspectives in silicon micro and nanophotonics. *Journal of the European Optical Society-Rapid publications*, *10*. doi: 10.2971/jeos.2015.15029

J2. Caliò, A., Cassinese, A., Casalino, M., Rea, I., Barra, M., Chiarella, F., & De Stefano, L. (2015). Hybrid organic–inorganic porous semiconductor transducer for multi-parameters sensing. *Journal of The Royal Society Interface*, *12*(108), 20141268. doi: 10.1098/rsif.2014.1268

J1. Caliò, A., Rea, I., Politi, J., Giardina, P., Longobardi, S., & De Stefano, L. (2013). Hybrid bio/non-bio interfaces for protein-glucose interaction monitoring. *Journal of Applied Physics*, *114*(13), 134904. doi: 10.1063/1.4824379

Proceedings

P7. Rea, I., Terracciano, M., Politi, J., **Caliò, A.**, Dardano, P., Gioffrè, M., Lamberti, A.,

Rendina, I., & De Stefano, L. (2015, October). Natural and synthetic nanostructured materials for biomedical applications. In *2015 AEIT International Annual Conference (AEIT)*(pp. 1-6). IEEE. doi:10.1109/AEIT.2015.7415279

P6. Caliò, A., Cassinese, A., Casalino, M., Politi, J., Barra, M., & De Stefano, L. (2015, May). Hybrid organic-inorganic semiconductor transducer for optical and electrical sensing. In *SPIE Optics+Optoelectronics* (pp. 95061R-95061R). International Society for Optics and Photonics. doi:10.1117/12.2178017

P5. Politi, J., **Caliò, A.**, Dardano, P., Iodice, M., Rea, I., & De Stefano, L. (2014). Bioconjugation of heavy metal-binding proteins on surface: an optical and gravimetric characterization. *Procedia Engineering*, *87*, 292-295. doi:10.1016/j.proeng.2014.11.665

P4. Caliò, A., Politi, J., Rea, I., & De Stefano, L. (2014, May). Hydrophobin-glucose interaction monitored by porous silicon optical multi-layers hybrid interfaces for sugar-proteins interaction monitoring. In *Photonics Technologies, 2014 Fotonica AEIT Italian Conference on* (pp. 1-4). IEEE. doi:10.1109/Fotonica.2014.6843956

P3. Caliò, A., Cassinese, A., Barra, M., Rea, I., & De Stefano, L. (2014, May). PDIF-CN_2 modified porous silicon optical and electrical transducers for biochemical sensing electrical and optical sensing by porous silicon devices. In *Photonics Technologies, 2014 Fotonica AEIT Italian Conference on* (pp. 1-4). IEEE. doi:10.1109/Fotonica.2014.6843900

P2. Rea, I., **Caliò, A.**, Terracciano, M., Politi, J., De Stefano, L., & Rendina, I., Porous silicon based photonic structures for optical monitoring of biochemical interactions. In *Fotonica 2013, 15° Convegno Nazionale delle Tecnologie Fotoniche*, Milano, 21-23 May 2013. ISBN 9788887237160, ISBN-A 10.978.8887237/160

P1. De Stefano, L., **Caliò, A.**, Politi, J., Giardina, P., Redina, I., & Rea, I. (2013, May). Hybrid interfaces for a new class of optical biosensors. In *SPIE Optics+Optoelectronics* (pp. 87741G-87741G). International Society for Optics and Photonics. doi:10.1117/12.2017615

È la volontà che fa l'uomo grande o piccolo.

Johann Christoph Friedrich von Schiller